AD_____

AWARD NUMBER: DAMD17-02-1-0679

TITLE: Driving Neurofibroma Formation in Mice

PRINCIPAL INVESTIGATOR: Nancy Ratner, Ph.D.

CONTRACTING ORGANIZATION: Children's Hospital Research Foundation
Cincinnati, Ohio 45229-3039

REPORT DATE: August 2006

TYPE OF REPORT: Final

PREPARED FOR: U.S. Army Medical Research and Materiel Command
Fort Detrick, Maryland 21702-5012

REPORT DOCUMENTATION PAGE

Form Approved
OMB No. 0704-0188

1. REPORT DATE *(DD-MM-YYYY)*	**2. REPORT TYPE**	**3. DATES COVERED** *(From - To)*
01-08-2006	Final	15 Jul 2002 – 14 Jul 2006

4. TITLE AND SUBTITLE

Driving Neurofibroma Formation in Mice

5a. CONTRACT NUMBER

5b. GRANT NUMBER
DAMD17-02-1-0679

5c. PROGRAM ELEMENT NUMBER

6. AUTHOR(S)

Nancy Ratner, Ph.D.

E-Mail: nancy.ratner@cchmc.org

5d. PROJECT NUMBER

5e. TASK NUMBER

5f. WORK UNIT NUMBER

7. PERFORMING ORGANIZATION NAME(S) AND ADDRESS(ES)

Children's Hospital Research Foundation
Cincinnati, Ohio 45229-3039

8. PERFORMING ORGANIZATION REPORT NUMBER

9. SPONSORING / MONITORING AGENCY NAME(S) AND ADDRESS(ES)
U.S. Army Medical Research and Materiel Command
Fort Detrick, Maryland 21702-5012

10. SPONSOR/MONITOR'S ACRONYM(S)

11. SPONSOR/MONITOR'S REPORT NUMBER(S)

12. DISTRIBUTION / AVAILABILITY STATEMENT
Approved for Public Release; Distribution Unlimited

13. SUPPLEMENTARY NOTES
Original contains colored plates: ALL DTIC reproductions will be in black and white.

14. ABSTRACT

Benign peripheral nerve tumors called neurofibromas are a major burden for patients with neurofibromatosis type 1 (NF1). No drug therapy is currently available for neurofibromas. Some Schwann cells in neurofibromas aberrantly express the epidermal growth factor receptor, making EGFR a possible therapeutic target. To test this, we used a novel transgenic mouse line in which the human EGFR is expressed in Schwann cells and in which nerve ultrastructure shows features of neurofibroma formation including Schwann cell hyperplasia, nerve hypertrophy, collagen deposition, and axon-glial disruption. We used the mAb Cetuximab (IMC-C225) to block human EGFR function in these mice and assessed nerve hypertrophy, mast cell accumulation, collagen deposition and axon-glial interactions normal at 3 months age. Hot plate sensory tests and electron microscopy confirmed histology data. To ascertain whether EGFR is necessary for malignant tumor formation in NF1, NPCis mice were mated to an EGFR hypomorph. The results of these studies suggest that EGFR acquisition is a key driving force for tumorigenesis in NF1.

15. SUBJECT TERMS
Schwann Cell, Neurofibroma, EGFR, NF1, Therapeutics

16. SECURITY CLASSIFICATION OF:			**17. LIMITATION OF ABSTRACT**	**18. NUMBER OF PAGES**	**19a. NAME OF RESPONSIBLE PERSON**
a. REPORT	**b. ABSTRACT**	**c. THIS PAGE**			USAMRMC
U	U	U	UU	57	**19b. TELEPHONE NUMBER** *(include area code)*

Table of Contents

INTRODUCTION

Nearly all (95%) of NF1 patients develop neurofibromas, benign Schwann cell tumors (Huson, 1994). The lifetime risk of NF1 patients for developing malignant peripheral nerve sheath tumors (MPNSTs), mainly from within plexiform neurofibromas, is 8-13% (Husan, 1994; Gutmann et al., 1997; Woodruff, 1999; Korf, 1999; Creange et al., 1999). Development of novel, non-surgical treatments to either prevent tumor formation or inhibit neurofibroma growth is a high priority. EGFR plays a very important role in tumor formation and prognosis (Salomon et al., 1995). The intensive study of EGFR signaling mechanisms has already yielded therapeutic agents in the treatment of cancer including antisense oligonucleotides (Mendelsohn and Baselga., 2000; Ciardiello and Tortora, 2001; Hirao et al., 1999; Ma et al., 1999) and small molecule inhibitors of enzymes (Discafani et al., 1999; Moasser et al., 2001; Shawver et al., 2002; Arteaga, 2003; Nutt et. al., 2004). Another therapeutic strategy is the use of monoclonal antibody (mAb) against the extracellular domain of the EGFR (Yang et al., 1999; Baselga et al., 2000). Among these is the mAb cetuximab (IMC-C225) (ImClone Systems, Inc., New York, NY). IMC-C225 is a human-specific EGFR monoclonal antibody currently in Phases II and III clinical testing in a number of EGFR overexpressiing cancers (Baselga et al., 2000; Barbara et al., 2002). It binds to the EGF receptor extracellular domain with high affinity, blocks ligand binding and down-regulates receptor expression on the cell surface (Kawamoto et al., 1983; Fan et al., 1993; Karashima et al., 2002; Sclabas et al., 2003). Normal Schwann cells lack EGFR expression. Expression of EGFR in some $S100^{+}$ neurofibroma cells and some cells in human MPNSTs (DeClue et al., 2000), in human MPNSTs cell lines and cell lines derived from compound heterozygous mice bearing loss of function in *Nf1* and *p53* suggest that EGFR could be an attractive target for the treatment of neurofibroma. To begin to test this idea we developed a mouse model in which human EGFR is expressed in peripheral nerve Schwann cells. In this contract we proposed to characterize this model, and to use it to test novel targeted therapeutic approaches including the mAb IMC-C225 and an anti-fibrotic, pirfenidone.

BODY

Task 1: Analysis of EGFR-expressing mouse.

- **a.** Define abnormalities in EGFR-overexpressing mouse nerves (Year 1).
- **b.** Evaluate effects of: a specific EGFR receptor antagonist **and**
- **c.** an anti-fibrotic drug, pirfenidone (Year 3).

Overall progress: Tasks 1a and 1b are complete; data is published. Task 1c is in progress.

hEGFR expression, dimerization, and activation in transgenic mice

To test the role of EGFR in neurofibroma formation, we developed transgenic mice in which the 2'3'-cyclic nucleotide 3' -phosphodiesterase (CNP) promoter, specific for Schwann cells in peripheral nerve (Chandross et al., 1999; Gravel et al., 1998; Tsukada and Kurihara et al., 1992; Weissbarth et al., 1991), drives expression of human EGFR. We raised and bred four founder mice, and confirmed presence of the hEGFR transgene in two lines, designated #10 and #46. Transgene integration effects are unlikely as two independent lines of mice demonstrated pathology described below. We confirmed hEGFR protein expression with monoclonal anti-human EGFR antibody to probe Western blots after immunoprecipitation with a polyclonal anti-EGFR antibody (Fig. 1*a*). We detected robust hEGFR expression using the same method in brain and spinal cord, where CNP drives expression in oligodendrocytes, with only trace expression in non-nervous tissues (Fig. 1*b* and *c*). We also detected hEGFR in sciatic nerve lysates from transgenic but not wild type mice (Fig. 1*d*, left side); RPMC cells served as a positive control. hEGFR expression levels were measured in lysates from Schwann cells purified from hEGFR expressing mouse nerves by Western blotting. The levels were less than those in 3 independent *p53;Nf1* cell lines (Li et al., 2002) (data not shown).

Ligand binding to the EGFR causes receptor autophosphorylation which leads to receptor activation as docking sites are created for signaling proteins (Prenzel et al., 2001). To test if expressed hEGFR in the transgenic mice is activated, we probed western blots of sciatic nerve lysates precipitated with anti-

human EGFR antibodies with an anti-phospho-EGFR antibody (Santa Cruz Biotech, Santa Cruz, California). EGF receptor in EGFR stimulated human RPMC cells was used as a positive control. Sciatic nerve lysates from CNP-hEGFR mice contained phosphorylated hEGFR, (Fig. 1*d*, right side) while lysates from wild type nerves did not (not shown). Consistent with a low level of phosphorylated EGFR we found no detectable changes in basal Ras-GTP or AKT-phosphorylation in Schwann cells from the mutant nerves as compared to wild type cells (data not shown).

Ligand binding to EGFR can induce homodimerization, or heterodimerization with ErbB2 or ErbB4 (Prenzel et al., 2001; Murali et al., 1996). Receptor dimerization is necessary for receptor activation. Schwann cells do not express ErbB4. We tested if hEGFR/ErbB2 dimers are present in nerves from transgenic mice. HEGFR formed no detectable heterodimers with ErbB2 in nerve lysates, although we easily detected dimers in lysates from RPMC cells (Fig. 1*e*). Thus, hEGFR likely exists as homodimers in CNP-hEGFR nerve. EGFR depends on ligands for homodimerization and activation (Prenzel et al., 2001). We analyzed expression of EGFR ligands in wild type and CNP-hEGFR sciatic nerves by quantitative real time PCR. We detected betacellulin, HB-EGF, and TGF-α in wild type and CNP-hEGFR nerves at approximately equivalent levels. No message was detected for EGF, epiregulin, or amphiregulin (Table 1). Schwann cells purified and expanded in culture expressed betacellulin and amphiregulin, confirming that peripheral glia make EGFR ligands (Table 1). The data are consistent with locally available ligands activating hEGFR receptors.

The CNP promoter drives expression in Schwann cells in peripheral nerve and oligodendrocytes in the central nervous system (Gravel et al., 1998). We stained sections of mouse nervous system for hEGFR using a species specific anti-human EGFR antibody. Oligodendrocytes were labeled in spinal cord (not shown). We detected no defects in brain sections, possibly due to unavailability of EGFR ligands in the brain. In saphenous nerve we detected labeling of myelinating Schwann cell sheaths, and inter-axon endoneurium staining suggestive of non-myelinating Schwann cell (NMSC); perineurium was

not labeled (Fig. 1*f*). We found no staining of wild type nerve (Fig. 1*h*) as compared to the much larger hEGFR saphenous nerve (Fig. 1*g*).

Nerves of CNPase-EGFR mice are enlarged.

Neurofibromas enlarge nerves in NF1 patients. Gross inspection of intercostal nerves, sciatic nerves, cauda equina, and cutaneous nerve twigs indicated diffuse hypertrophy in all CNP-hEGFR transgenic mice (not shown). We gathered quantitative data on nerve size in saphenous nerve. Sapphenous nerves are easily accessible in dissections and maintain a constant diameter, without branches, over a lengthy segment. We measured nerve cross-sectional area (Fig. 2*a*). We noted a significant up to 8-fold increase in area of transgenic nerves in comparison to wild-type nerves ($P = 0.001$). Hypertrophy was also noted in trigemminal nerves of transgenic mice (Fig. 2*b*).

CNPase-EGFR; *Nf1*$^{+/-}$ mice do not show evidence of worsening pathology

Loss of function of *Nf1* in Schwann cells cooperates with *Nf1*$^{+/-}$ in other cells in one model (Zhu et al., 2002). To examine if *Nf1*$^{+/-}$ worsened the CNP-hEGFR nerve phenotype, we bred CNP-hEGFR mice with *Nf1*$^{+/-}$ mice. Dissection along the neuroaxis and peripheral nervous system of double heterozygous mice revealed similar diffuse nerve enlargement as in CNP-hEGFR mice. Saphenous nerves of 4 double-heterozygous mice were significantly larger ($P = 0.0075$) compared to wild-type mice, but not significantly different ($P = 0.41$) from nerves of mice which were only EGFR positive (Fig. 2*a*; triangles).

Increased nuclei in CNPase-hEGFR nerves.

The histological basis of the nerve hypertrophy in CNP-hEGFR mice is attributable at least in part to hypercellularity. We counted nuclei in hemotoxylin stained nerve cross-sections and found them increased 2 – 8-fold in hEGFR nerves ($P = 0.01$, Fig. 2*c*). In contrast, there was no significant change in number of myelinated axons: wild-type saphenous nerves harbored on average 465 large axons, while transgenic nerves averaged 499 (n = 3 each; $P = 0.32$). Increased numbers of endoneurial cells in mutant nerves could result from increased proliferation and/or decreased cell death. We analyzed entry into S-

phase of endoneurial cells in mutant nerves by labeling with BrdU. In wild-type adult nerves, we detected the expected low proliferation rate (0.4%) in 6 hours (Brown and Asbury, 1981). While the absolute numbers of BrdU positive nuclei were higher in transgenic nerves, the ratio of positive nuclei to total nuclei was not significantly different ($P = 0.96$) (Fig. 3*e*). We analyzed cell death as measured by TUNEL positive nuclei. We found 0.4% TUNEL positive nuclei in wild-type nerves (Grinspan et al., 1996); numbers of positive nuclei in transgenic mice were not significantly different ($P = 0.16$, Fig. 3*f*). Thus ongoing increases in cell proliferation or decreased cell death are not present in adult nerves, suggesting cell number increases at earlier times (see below). Neurofibroma cells also show little proliferation and death (Kourea et al., 1999).

Hyperplastic endoneurial cells in transgenic nerves might be Schwann cells, fibroblasts, and/or perineurial cells; each is present at variable levels in neurofibromas. Wild type and CNPase-hEGFR nerve cells associated with myelin sheaths showed cytoplasmic S100 positive staining as expected for myelinating Schwann cells (Mata et al., 1990; Fig. 3*a* and *c*) and p75NGFR immunoreactivity characteristic of non-myelin-forming Schwann cells (NMSCs) (Fig. 3*b* and *d*). Greater than 90% of nuclei unassociated with myelin sheaths were surrounded by GFAP-positive cytoplasm, supporting a NMSC phenotype (Jessen et al., 1990; not shown). Continuous basal lamina characteristic of Schwann cells was present on >90% of cells in the endoneurium of CNPase-hEGFR saphenous nerves in electron micrographs (Fig. 3*g* and *h*). Most endoneurial cells are therefore Schwann cells; others may be fibroblasts or perineurial cells.

Unmyelinated fiber bundles and non-myelinating Schwann cells in CNPase-EGFR mice exhibit marked alterations which worsen distally and with time

We analyzed electron micrographs to define nerve pathology. Normal 4 month-old saphenous nerve contains large axons surrounded by single myelin-forming Schwann cells and groups of smaller axons ensheathed together by individual NMSCs (Fig. 4*b*). The same age transgenic saphenous nerves

were abnormal (*n*=5) (Fig. 4*a*, *c*-*e*). NMSCs displayed long aberrant processes which wrapped one or two, or no, small axons. . Collagen fibers filled the nerve matrix between large myelinated axons and were frequently, errantly, "wrapped" by Schwann cell processes (Fig. *3h*, 4*e* inset). Notably, many Schwann cells in neurofibromas lack contact with axons.

The increased size of CNPase-hEGFR nerve results from an increase in the number of nerve Schwann cells (Fig. 2), increased collagen and increased myelin thickness. We measured myelin sheath thickness (*n*=100) and the distance between myelin sheaths (*n*=100) in electron micrographs from 3 wild type and 3 CNPase-hEGFR saphenous nerves. Both parameters were increased (*P*<.0001; Wilcoxon non-parametric test).

We observed a proximal to distal worsening of phenotype. We examined sciatic and saphenous nerves in the same mice at 4 months of age (*n*=2). Sciatic nerves had nearly normal appearing small axonal fiber bundles when saphenous nerves had NMSCs with aberrant processes. Saphenous nerve pathology also worsened with time. Our cohort studied by EM included 2-month old (*n*=2), 4-month (*n*=5), and 6-month old (*n*=2) transgenic mice. Nerves progressively accumulated collagen, dysfunctional Schwann cells, and had increasing numbers of disrupted small axonal fiber bundles (Fig. 4*f*-*h*). These patterns of pathology suggest a dying-back neuropathy of small caliber axons.

CNP-EGFR nerves exhibit increased mast cell infiltration and fibrosis

Neurofibromas contain more mast cells than normal nerve (Johnson et al., 1989). We observed granule-laden mast cells in electron micrographs of hEGFR nerves (Fig. 5*a*). We counted mast cells in saphenous nerve cross-sections (Fig. 5*b*). Mast cell numbers were significantly increased in transgenic nerves (*P* = 0.004) (Fig. 5*c*). Many mast cells were degranulating. Mast cell chemoattractants BDNF, MCP-1, SCF, and TGF-β1, were each up-regulated in mutant nerves as determined by Q-RTPCR (Fig 5*d*), likely accounting for the additional mast cells. Schwann cell hyperplasia precedes mast cell accumulation; in 4-week-old mouse hEGFR sciatic nerve Schwann cell numbers were significantly

increased ($P<0.0001$) (Fig. 5*e*), but mast cell numbers were not (Fig. 5*f*). Sciatic nerves were studied in developing animals as saphenous nerves were too small to reliably embed at this age. Mast cell products induce fibrosis, and we confirmed enhanced collagen accumulation by trichrome stain in adult sapphenous nerve (Fig, 5*g*,*h*), but not 4-week-old sciatic nerves (data not shown).

hEGFR mice develop rare nerve tumors

We aged 19 hEGFR and 12 wild type littermates until moribund. EGFR mice (42%) and 50% of wild type mice remain alive at 23 months. We observed nerve thickening in 11 EGFR mice evaluated at autopsy, but found no consistent cause of death. We observed a grossly enlarged spinal nerve root in one mouse diagnosed as a neurofibroma (Fig 6*a*). Another mouse developed nerve-associated spindle cell tumor with muscle differentiation (Fig 6*b*). Desmin and S100 staining (Fig 6*c*,*d*) were positive confirming a diagnosis of triton tumor. We used an anti-human EGFR antibody to probe western blots after immunoprecipitation of brain and tumor lysates from this mouse with a polyclonal anti-EGFR antibody (Fig. 6*e*). hEGFR was enriched in the tumor demonstrating transgene association. We analyzed six EGFR/*Nf1*$^{+/-}$ mice. Nerve thickening was consistent but no nerve tumors were detected and no consistent cause of death found. These data suggest that EGFR expression can lead to peripheral nerve tumorigenesis, benign and malignant, but that frank tumor formation in this model is rare, even when mice are hemizygous for *Nf1* mutation.

EXPERIMENTAL PROCEDURES

Generation of CNPase-hEGFR transgenic mice.

We subcloned the 2'3'-cyclic nucleotide 3'-phosphodiesterase (CNP) promoter (Chandross et al., 1999) into a Bluescript (Stratagene, La Jolla, CA) backbone. We inserted the human EGFR cDNA (Velu et al., 1987) into SstII and XhoI sites in the newly created multiple cloning site downstream of the promoter. We confirmed sequence integrity by DNA sequencing (UC sequencing core facility). We

excised the promoter, EGFR cDNA, and SV40 polyadenylation signal with VspI and MluI.and injected it into C57BL/6 – SJL hybrid mouse oocytes.

hEGFR localization.

We prepared tissue extracts using 10ul buffer (1% triton X100, 50 mM Tris pH 7.4, 150 mM NaCl, 1ug/mL aprotinin, 1 ug/mL leupeptin, 1 ug/mL pepstatin, 1 mM PMSF) /mg tissue. We incubated lysates with at 4°C overnight with goat polyclonal anti-EGFR (Santa Cruz sc-03g; Sandta Cruz, CA) and then with protein A/G agarose beads (Santa Cruz). We subjected samples to SDS-PAGE on 4-20% gradient gels, and probed blots with human specific mouse monoclonal anti-EGFR (Zymed; South San Francisco, CA) or with anti-phosphorylated EGFR (Santa Cruz). We developed blots using an enhanced chemiluminescence kit (Amersham/Pharmacia; Piscataway, NJ).

We studied EGFR dimer formation by immunoprecipitation using a human-specific mouse monoclonal anti-EGFR (Upstate Biotech #05-101, Lake Placid, NY). We ran 8% SDS-PAGE gels and probed blots with anti-ErbB2 (Oncogene Research c-neu; Cambridge, MA) or anti-hEGFR (Zymed). We used the RPM-MC human melanoma cell line known to express ErbB2 and EGFR as a positive control. Schwann cells were prepared as described in Kim et al. (1995). EGFR expression and AKT phosphorylation were as described in Li et al. (2002). *p53;Nf1* cell lines tested were 61D-20, 38-2-15-L53 and 32-8-38. Ras activation assays were done as recommended by the manufacturer (Upstate Biologicals).

Immunohistochemistry and histology.

We sacrificed mice by perfusion fixation with 4% paraformaldehyde and harvested sciatic and saphenous nerves. We embedded nerves in paraffin and cut 6μm thick cross-sections; every fifth section was mounted to avoid double counting. We analyzed sciatic nerve sections proximal to the sciatic bifurcation. We stained sections with hematoxylin for nuclear counts, toluidine blue for mast cells, and Gamori's trichrome for collagen.

We stained paraffin sections using a human-specific mouse monoclonal anti-EGFR (Zymed). Sections were first blocked for one hour using the Zymed Histomouse kit. We used rabbit polyclonal anti-cow S100 (Dako, Carpenteria, CA) and anti p75 (Chemicon, Teincula, CA). For fluorescence microscopy we used Alexa-488 fluorescent conjugated anti-rabbit secondary and counterstained with bisbenzamide (DAPI) to identify nuclei.

Schwann cell proliferation and apoptosis

We gave mice three intraperitoneal BrdU injections (0.05mg/gm) at 2 hour intervals. We sacrificed mice, harvested nerves, and cut paraffin sections. We detected BrdU uptake with biotinylated anti-BrdU antibody (Zymed) followed by incubation with streptavidin-conjugated rhodamine (Jackson ImmunoResearch Corp; West Grove, PA). To quantify cell death, we used the TdT-FragEL DNA Fragmentation Detection Kit (Oncogene Research Products). We counted nuclei with DAPI co-staining.

Examination of nerve ultrastructure

We perfusion fixed anaesthetized mice with 3.2% glutaraldehyde with 3% paraformaldehyde in 0.1M cacodylate buffer for 10 minutes, followed by postfixation *in situ* for 20 min. We harvested sciatic and saphenous nerves, rinsed them with 0.1M phosphate buffer, post-fixed with 2% osmium tetroxide and 0.6% potassium ferrocyanide, and embedded them in Embed plastic. We stained semi-thin sections (1μM) with toluidine blue to count of myelinated axons by light microscopy. We viewed thin sections stained with uranyl acetate and lead citrate on a Jeol 100CX electron microscope.

Detection of EGFR ligands and mast cell chemoattractants by quantitative real time PCR

We extracted messenger RNA was from wild-type and CNPase-hEGFR mouse sciatic nerves, or from mouse Schwann cells isolated as described (Kim et al., 1995), using the Micro-FastTrack^{TM} kit (Invitrogen; Carlsbad, CA). We reverse transcribed mRNA using the Superscript Preamplification System (GibcoBRL; Grand Island, NY) with Superscript II reverse transcriptase, oligo-dT primers and random hexamers per manufacturer's protocol. We controlled for genomic DNA contamination by

omitting reverse transcriptase. We amplified GAPDH as a control (sense, 5'-ACCCAGAAGACTGTGGATGG-3' and antisense, 5'-GGAGACAACCTGGTCCTCAG-3'; product size, 300 bp) for each sample. We carried out quantitative real-time PCR experiments in the presence of SYBR green using the primers: amphiregulin (AR; sense, 5'-TGGCAGTGAACTCTCCACAG-3' and antisense, 5'-CAATTGCATGTCACCACCTC-3'; product size, 300 bp), betacellulin (BTC; sense, 5'-GGAACCTGAGGACTCATCCA-3' and antisense, 5'-TCTAGGGGTGGTACCTGTGC-3'; product size, 227 bp), epidermal growth factor (EGF; sense, 5'-GAGAGGTGCAGAAGGACCTG-3' and antisense, 5'-CACCAATTGCTGGTGATTTG-3'; product size, 271 bp), epiregulin (EPREG; sense, 5'-TTCAGATGGAAGACGATCCC-3' and antisense, 5'-CGCAACGTATTCTTTGCTCA-3'; product size, 206 bp) heparin-binding EGF (HBEGF; sense, 5'-ATAGCTTTGCGCTGTGACCT-3' and antisense, 5'-CACACTCTTTGGTCCCACCT-3'; product size, 166bp), and transforming growth factor-β (TGFβ; sense, 5'-TGTGTGATAAAGCTGCCTGC-3' and antisense, 5'-CAACCCTTTGAGGTTCGTGT-3'; product size, 100 bp). To determine differential expression of mast cell chemoattractants, the following primers sets were used: anaphylatoxin C3a (AnapC3a; sense, 5'-GGCTTCTTGTGTTGGTTGGT and antisense, 5'-AGCCAGGGCTACTGTCTTGA, product size, 131bp), anaphylatoxin C5a (AnapC5a; sense, 5'-CTACCATTAGTCCCGACCGT and antisense, 5'-AGAGGCAACACAAAACCCAC, product size, 265bp), brain derived neurotrophic factor (BDNF; sense, 5'-TGGCTGCACTTTTGAGCAC and antisense, 5'-GCAGTCTTTTTATCTGCCGC, product size, 292bp), eotaxin (sense, 5'-CTCCACAGCGCTTCTATTCC and antisense, 5'-TTTGGAGTTTTTGGTCCAGG, product size, 272bp), fractalkine (sense, 5'- ATTTATTGGATTCCCAGCCC and antisense, 5'-CGGAGAGCTCCAGAAAACAC, product size, 284bp), interleukin-6 (IL-6; sense, 5'-AGTTGCCTTCTTGGGACTGA and antisense, 5'-TCCACGATTTCCCAGAGAAC, product size, 159bp), leukemia inhibitory factor (LIF; sense, 5'-CTGACTGCCTCCCACTTCTC and antisense, 5'-AGCCTTCCTCTCACTCCACA, product size, 170bp), monocyte chemoattractant protein 1 (MCP-1;

sense, 5'-AGCACCAGCCAACTCTCACT and antisense, 5'-CGTTAACTGCATCTGGCTGA, product size, 136bp) nerve growth factor (NGF; sense, 5'-GTGAAGATGCTGTGCCTCAA and antisense, 5'-TACGCTATGCACCTCACTGC, product size, 204bp), neurotrophin-3 (Ntf3; sense, 5'-GATCCAGGCGGATATCTTGA and antisense, 5'-AGCGTCTCTGTTGCCGTAGT, product size, 182bp), platelet activating receptor (PAR; sense, 5'-AGCAGAGTTGGGCTACCAGA and antisense, 5'-TGCGCATGCTGTAAAACTTC, product size, 164bp), rantes (sense, 5'-GTGCCCACGTCAAGGAGTAT and antisense, 5'- GGGAAGCGTATACAGGGTCA, product size, 186bp), serum amyloid A (SAA; sense, 5'-CTAGAGTCGATCTGCCCAGC and antisense, 5'-TCATGTCAGTGTAGGCTCGC, product size, 164bp), stem cell factor (SCF; sense, 5'-CAGTCTTCAGGAGTGAGCCC and antisense, 5'- CAAAGATGCTCCCAAACGCT, product size, 254bp), transforming growth factor β1 (TGF-β; sense, 5'-TGAGTGGCTGTCTTTTGACG and antisense, 5'- TCTCTGTGGAGCTGAAGCAA, product size, 293bp), and vascular endothelial growth factor (VEGF; sense, 5'- AGCCAACAGGGAATTTGATG and antisense, 5'-CACAGCGGCATACTTCTTCA, product size, 239bp). We preformed replicate reactions in an ABI Prism 7700 Sequence Detection System Cycler according to manufacturer's instructions. We confirmed all PCR products on 2% agarose gels. We calculated ΔC_t values relative to GAPDH expression. We calculated the fold changes in CNP-hEGFR nerves compared to wild type nerves using the equation: $2^{-\Delta\Delta Ct}$, where C_t is the cycle number at the chosen amplification threshold as determined by PE Biosystems software, $\Delta C_t = C_{t(ligand)} - C_{t(GAPDH)}$, and $\Delta\Delta C_t = \Delta C_{t(+/-)} - \Delta C_{t(+/+)}$ (K. Luvak, PE ABI Sequence Detector User Bulletin 2).

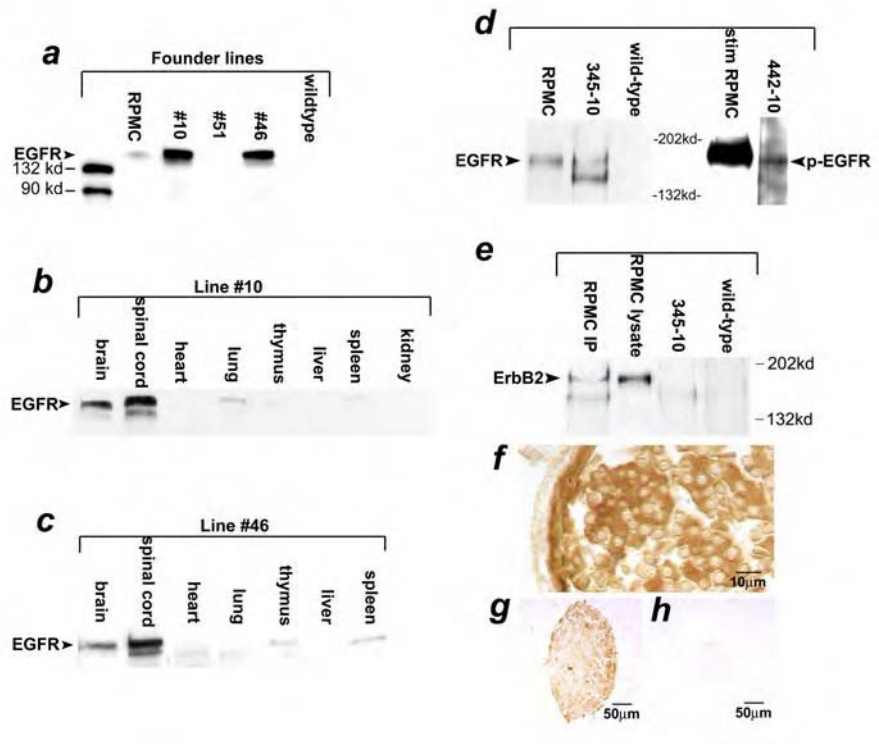

Fig. 1 Human EGFR protein is expressed in CNPase-hEGFR transgenic mice. ***a***, Western immunoblot of immunoprecipitates from brain lysates demonstrating protein expression of hEGFR in two transgenic founder lines. Positive control: RPMC cell line (human melanoma) known to express EGFR and ErbB2. Specific tissue expression of hEGFR demonstrated in line #10 (***b***) and line #46 (***c***) with expression seen predominantly in brain and spinal cord with trace expression in non-neural tissues. ***d***, Sciatic nerve expression of hEGFR confirmed with specimen 345-10, and demonstration of active phosphorylated EGFR seen in spinal cord lysate of specimen 442-10. Positive control: RPMC cells stimulated with EGF. ***e***, Demonstration of lack of heterodimer formation between hEGFR and ErbB2: lysates were immunoprecipitated with anti-hEGFR and blots probed for ErbB2. No band noted in specimen 345-10 as compared to positive control RPMC cells which do exhibit heterodimer formation. ***f***, Immunohistochemistry of saphenous nerve demonstrating cell-specific hEGFR expression with positive Schwann cell sheath staining and lack of axonal staining. Low magnification saphenous nerve staining for hEGFR in transgenic specimen (***g***) is compared to lack of staining in wild-type specimen (***h***).

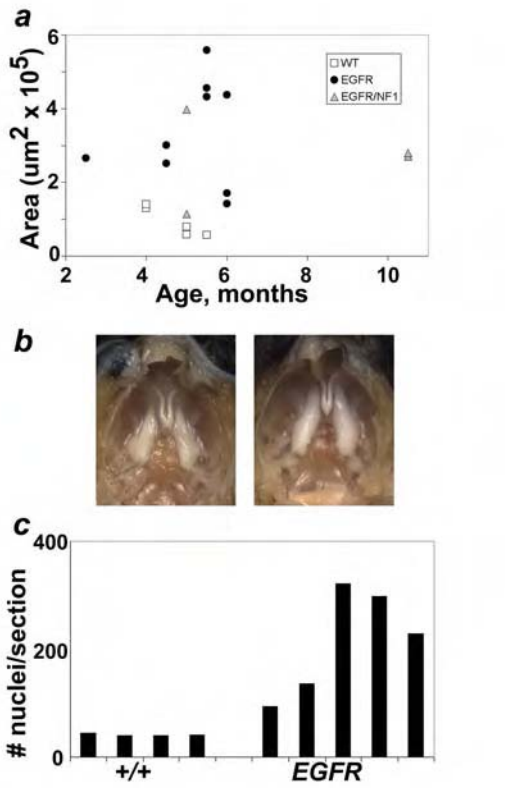

Fig. 2 CNPase-hEGFR nerves are enlarged and hypercellular. ***a***, Cross-sectional area of saphenous nerves plotted with respect to age and distinguished by genotype. Significant enlargement of CNPase-hEGFR and CNPase-hEGFR, *Nf1*$^{+/-}$ nerves compared to wild-type (*P*=0.001 and *P*=0.008 respectively) is seen. ***b***, Dorsal view of skull bases with brain removed demonstrating enlargement of trigeminal nerves; wild-type is shown on left, CNPase-hEGFR on right. ***c***, Nuclei counts from saphenous nerve cross-sections accomplished by hematoxylin staining. CNPase-hEGFR nerves have significantly increased nuclei (*P*=0.01).

Fig. 3 Hypercellularity is attributable to Schwann cells. ***a-d***, Markers for Schwann cells: S100 staining of saphenous nerve cross-sections in wild-type (***a***) and CNPase-hEGFR (***c***) mice, and p75 staining in wild-type (***b***) and CNPase-hEGFR (***d***) mice. ***e***, Assessment of BrdU uptake over 6 hours and ***f***, apoptosis rates by TUNEL staining in saphenous nerve cross-sections showing no significant difference between wild-type and CNPase-hEGFR nerves. ***g-h***, Electron micrographs: presence of a basal lamina (small arrows) around a non-myelinating Schwann cell and its ensheathed axons (Ax) in wild-type nerve (***g***). Basal lamina is present around Schwann cell membrane processes in a CNPase-hEGFR nerve.

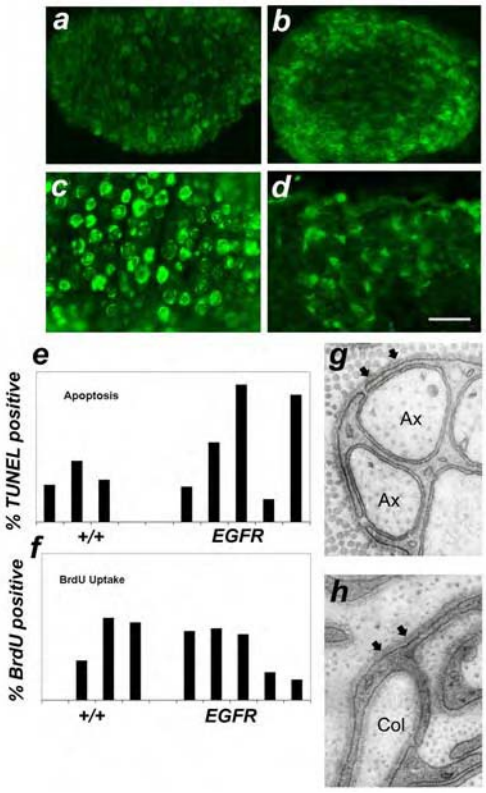

Fig. 4 Ultrastructural studies show pathology of CNPase-hEGFR nerves. a, Electron micrograph montage of CNPase-hEGFR saphenous nerve. b, In comparison, wild-type saphenous nerve at the same magnification

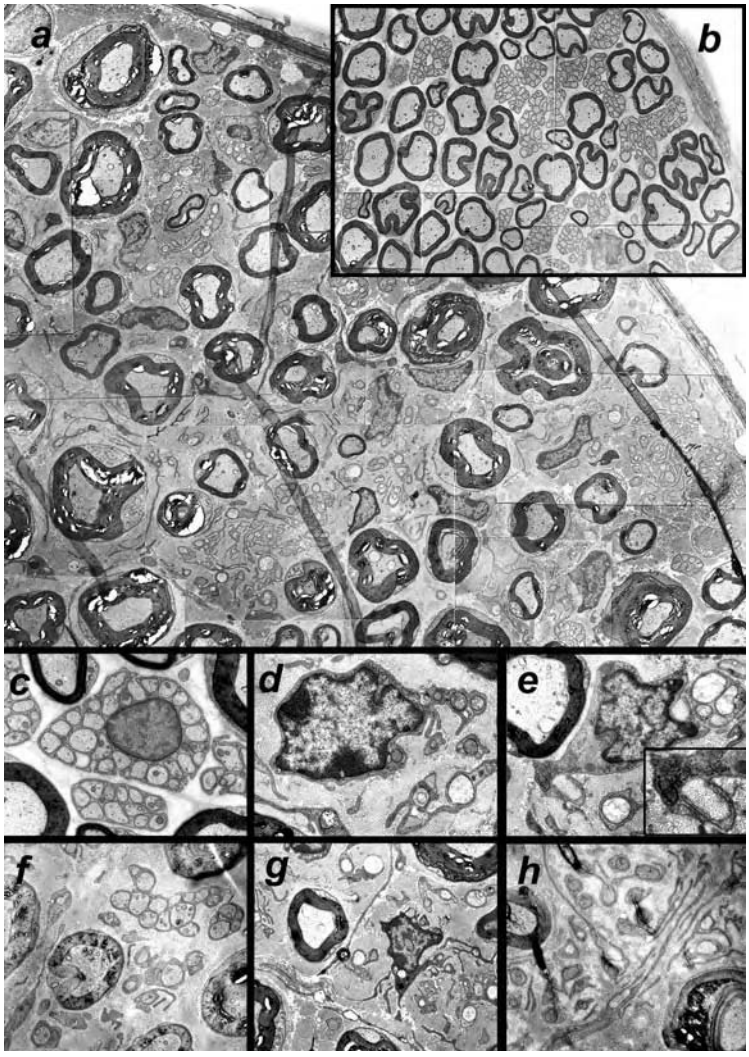

(4000X). c, A normal non-myelinating Schwann cell nucleus with cell membrane wrapping of small axons in wild-type nerve. d, A markedly dysmorphic nucleus in CNPase-hEGFR nerve with membrane wrapping of a limited number of axons, and e, another example showing Schwann cell processes with no association with any axons and pathologic wrapping of collagen fibrils (inset). Pathology is seen to progress with time in CNPase-hEGFR nerves comparing a 2.5 month-old specimen (f) to a 4 month-old specimen (g) and to a 6 month-old specimen (h). (c-h 10,000X; except g is 5333X).

Fig. 5 Mast cells and fibrosis in CNPase-hEGFR mouse nerves. a, Mast cell seen in CNPase-hEGFR saphenous nerve on electron micrograph magnified 8000X. b, Toluidine blue staining of CNPase-hEGFR saphenous nerve cross-section showing multiple metachromatic mast cells (arrows). c,f, Mast cell counts in saphenous nerves. c, Adult nerve comparing wild-type mice (+/+) to CNPase-hEGFR mice (EG) to CNPase-hEGFR;Nf1$^{+/-}$ mice (EG/NF). CNPase-hEGFR and CNPase-hEGFR;Nf1$^{+/-}$ nerves harbor significantly more mast cells (P=0.004 and P=0.015 respectively) than wild-type nerves. d, Differential expression of mast cell chemoattractants mRNA in adult hEGFR nerve as detected by real time-PCR. * = expressed only in hEGFR nerve. e, Total nuclei are increased in 4-week-old sciatic hEGFR nerves (P<0.0001).

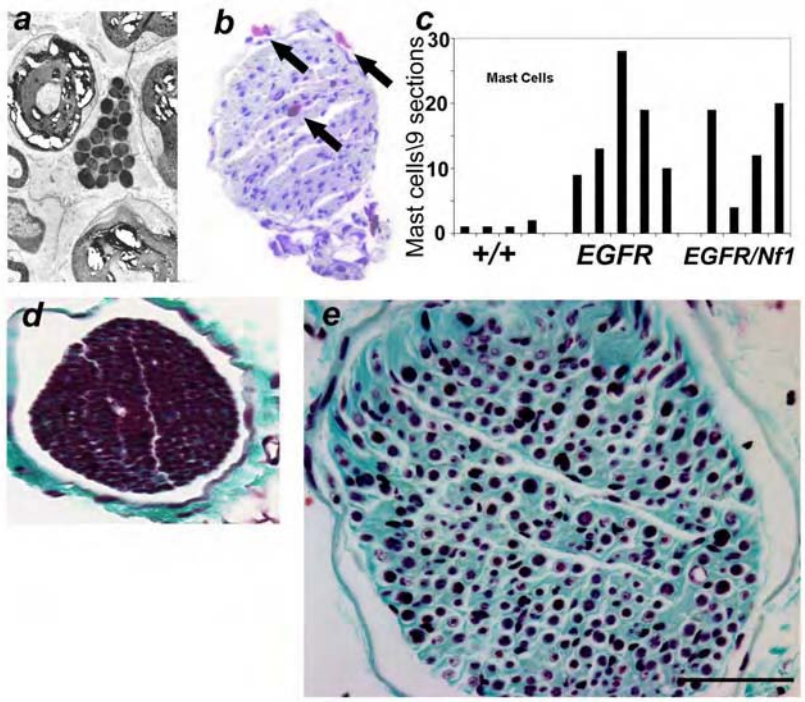

Fig. 6 Tumors of CNPase-hEGFR mouse nerves. **a**, Enlarged spinal nerve root, diagnosed as a neurofibroma, from CNPase-hEGFR mouse. **b**, Triton tumor from CNPase-hEGFR mouse (H&E). This was confirmed with S100 (**c**) and desmin (**d**) staining. **e**, Western immunoblot of immunoprecipitates of brain and triton tumor lysates from this mouse, demonstrating enriched hEGFR expression in the tumor. No expression of hEGFR is seen in a lipoma from the same mouse. **a-d,** Bar = 1000uM.

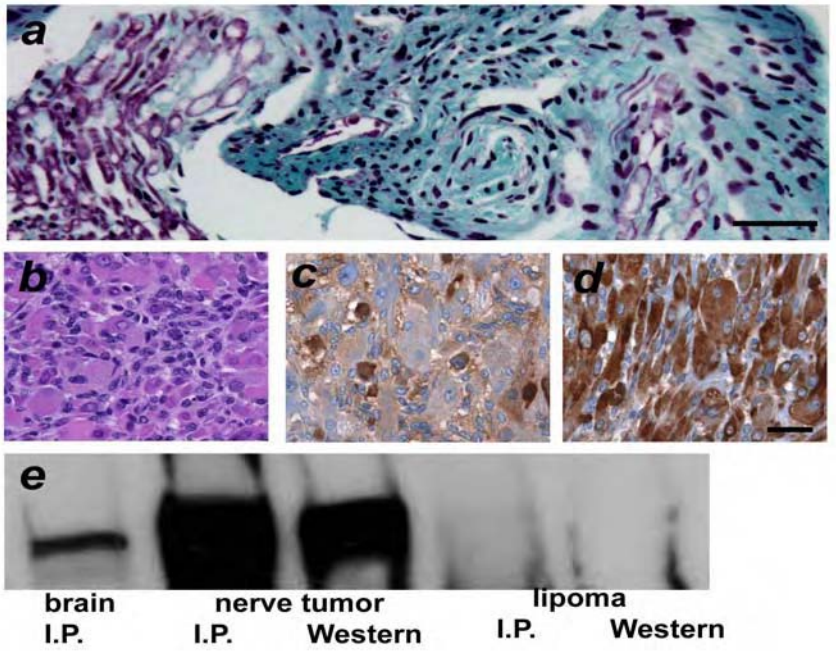

Table 1 Presence of EGFR ligand mRNA as detected by Real Time-PCR. WT = wild-type, MSC = mouse Schwann cells, AR = amphiregulin, BTC = betacellulin, EGF = epidermal growth factor, EPREG = epiregulin, HBEGF = heparin-binding epidermal growth factor, TGF-α = transforming growth factor α.

Table 1. mRNAs encoding EGFR ligands are present in adult peripheral nerve and cultured Schwann cells.

A. *Ligands*

	AR	***BTC***	***EGF***	***EPIREG***	***HBEGF***	***TGF-α***
WT Nerve	-	+	-	-	+	+
EGFR nerve	-	+	-	-	+	+
MSC	-	+	-	-	-	+

B. *Quantification of Ligands Present in Nerve*

BTC					
	BTC avg C_t	**GAPDH avg C_t**	**ΔC_t**	**$\Delta\Delta C_t$**	**Fold Change**
W/T	31.94 ± 0.02	25.46 ± 0.49	6.48 ± 0.49	0.00 ± 0.49	***1*** (0.71-1.41)
EGFR	27.90 ± 0.02	27.76 ± 0.15	5.14 ± 0.15	-1.34 ± 0.15	***2.53*** (2.28-2.81)
HBEGF					
	HBEGF avg C_t	**GAPDH avg C_t**	**ΔC_t**	**$\Delta\Delta C_t$**	**Fold Change**
W/T	31.42 ± 0.05	27.61 ± 0.50	3.81 ± 0.50	0.00 ± 0.60	***1*** (0.71-1.41)
EGFR	33.20 ± 0.23	30.35 ± 0.15	2.85 ± 0.27	-0.96 ± 0.27	***1.94*** (1.61-2.35
TGF-α					
	TGF-α avg C_t	**GAPDH avg C_t**	**ΔC_t**	**$\Delta\Delta C_t$**	**Fold Change**
W/T	29.00 ± 0.19	27.61 ± 0.50	1.39 ± 0.53	0.00 ± 0.53	***1*** (0.69-1.44)
EGFR	31.00 ± 0.23	30.35 ± 0.15	0.65 ± 0.27	-0.74 ± 0.27	***1.67*** (1.39-2.01)

Task 1b: Evaluate effects of an EGFR receptor antagonist, OSI EGFR

Last year we carried out 3 experiments using Wyeth EKI series drugs, which inhibit EGFR and the related ErbB2 tyrosine kinase. We found that dosing EGFR mice for 6 weeks, at 2 – 3.5 months of age was not

sufficient to reverse the nerve phenotypes—we assayed mast cell numbers, Schwann cell numbers and electron microscopy as described above. We then tried dosing mice at younger ages, as proposed in the grant. Mice were not able to survive the treatment—this was not unexpected as EGFR knockout mice die perinatally. To circumvent this difficulty we have initiated a new set of studies in which we treat mice with a humanized anti-human EGFR antibody (Erbitux). This does not react with mouse endogenous EGFR but inhibit function of the transgenic human EGFR.

Task 1b: Evaluate the therapeutic effect of EGFR antagonist (mAb Cetuximab) on EGFR mouse model.

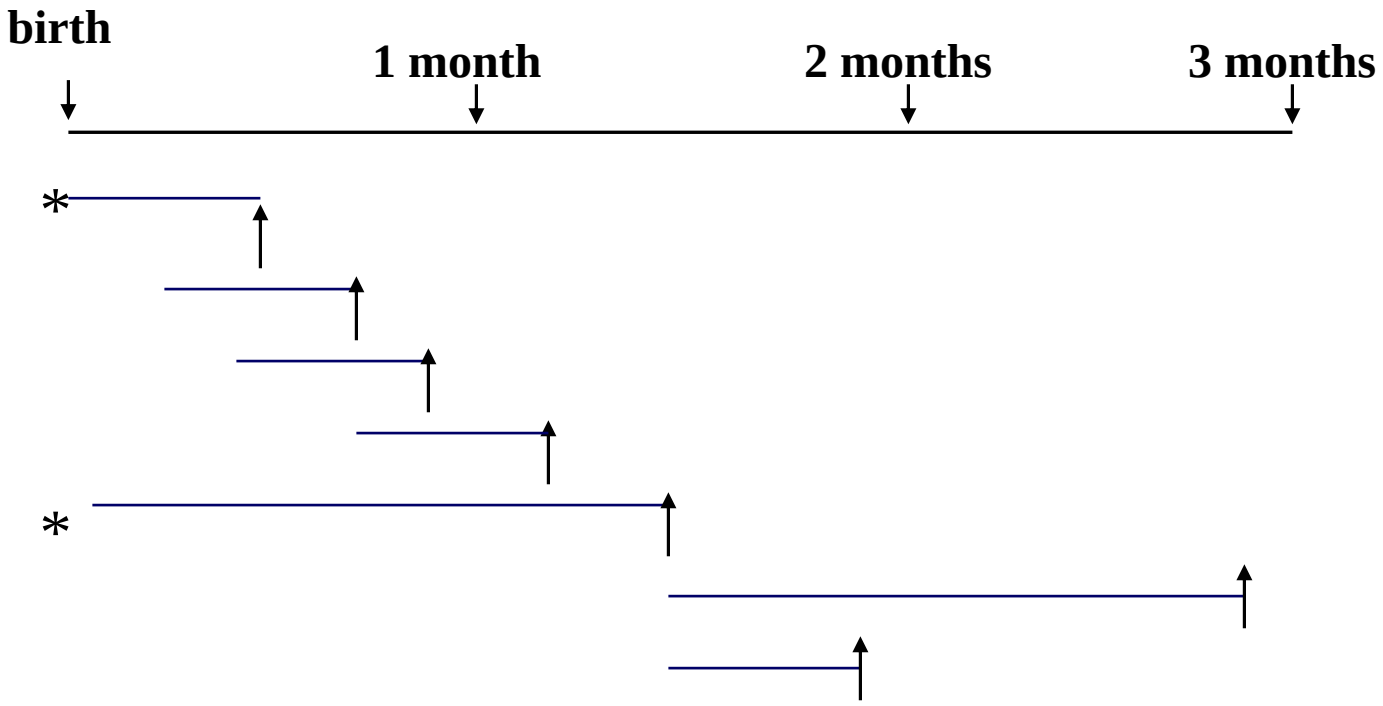

Fig.7. Schematic diagram of IMC-C225 injection into hEGFR transgenic mice.

IMC-C225 was injected (i.p.) twice weekly at a dose of 1mg/25g, the injection dose and volume was adjusted according to the mouse body weight. Control group was injected with same volume of PBS. 12-16 mice were in each group. Mice were sacrificed at 3 months of age. * shows IMC-C225 has effect on reversing the phenotype.

The hEGFR is phosphorylated in the CNPase-hEGFR transgenic nerve (see above). In order to determine whether IMC-C225 was capable of reaching nerve and inhibiting EGFR function, we treated newborn mice with IMC-C225 for two weeks, then assessed EGFR phosphorylation on sciatic nerve sections in this mouse model using an antibody specific for phosphorylated EGFR. As shown in Fig 8., hEGFR phosphorylation was robust surrounding sciatic nerve nuclei in untreated hEGFR mice. Phosphorylation decreased significantly after 2 week exposure to IMC-C225. Control experiments

showed that treatment had no effect on wild type mice as expected because IMC-225 does not inhibit rodent EGFR and because wild type mouse Schwann cells do not express EGFR (data not shown).

Fig. 8. IMC-C225 inhibits Schwann cell EGF**i**R phosphorylation in EGFR(+) mouse.

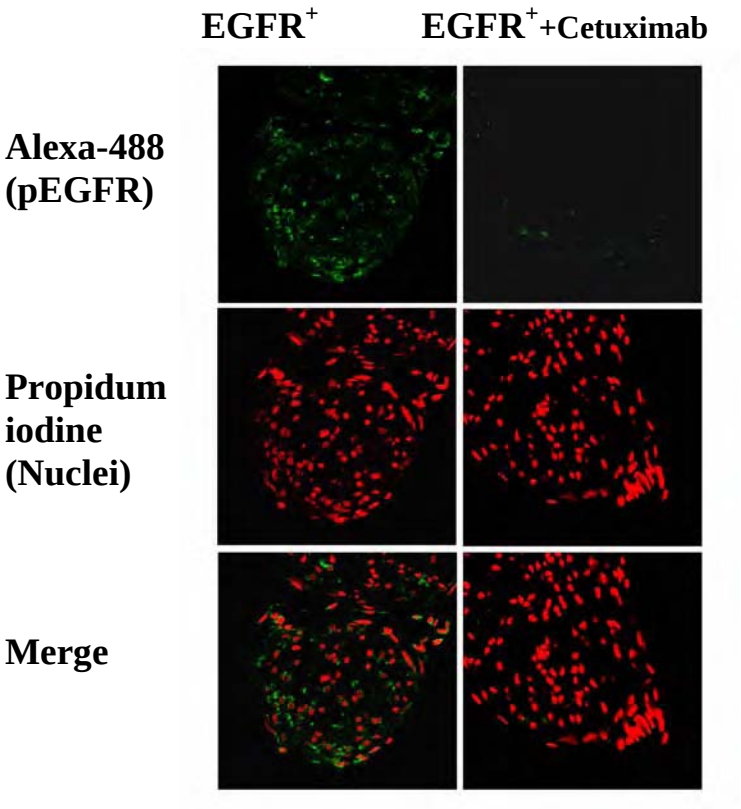

Mice were treated with IMC-C225 and immunfluorescence was performed as described in Material and methods. hEGFR phosphorylation was robust surrounding sciatic nerve nuclei in untreated hEGFR mice (left). Phosphorylation decreased significantly after 2 week exposure to IMC-C225 (right).

To test if the Schwann cell proliferation that occurs in mutant nerve was a direct consequence of hEGFR expression, we measured proliferation of nerve Schwann cells by BrdU incorporation after exposure to IMC-C225. We have previously shown that Schwann cell proliferation in this model is maximal in the 2 weeks after birth. Wild type or transgenic mice were treated with IMC-C225 or PBS twice a week over the first 2 postnatal weeks. BrdU was I.P. injected at 2 weeks of age before i.c. perfusion. Sciatic nerves were analyzed for cell proliferation and nuclei counting. As shown in Fig 9, the number of BrdU-labeled nuclei in the sciatic nerve of hEGFR mice was more than 3 fold higher than in wild type mouse littermates.

Fig 9A

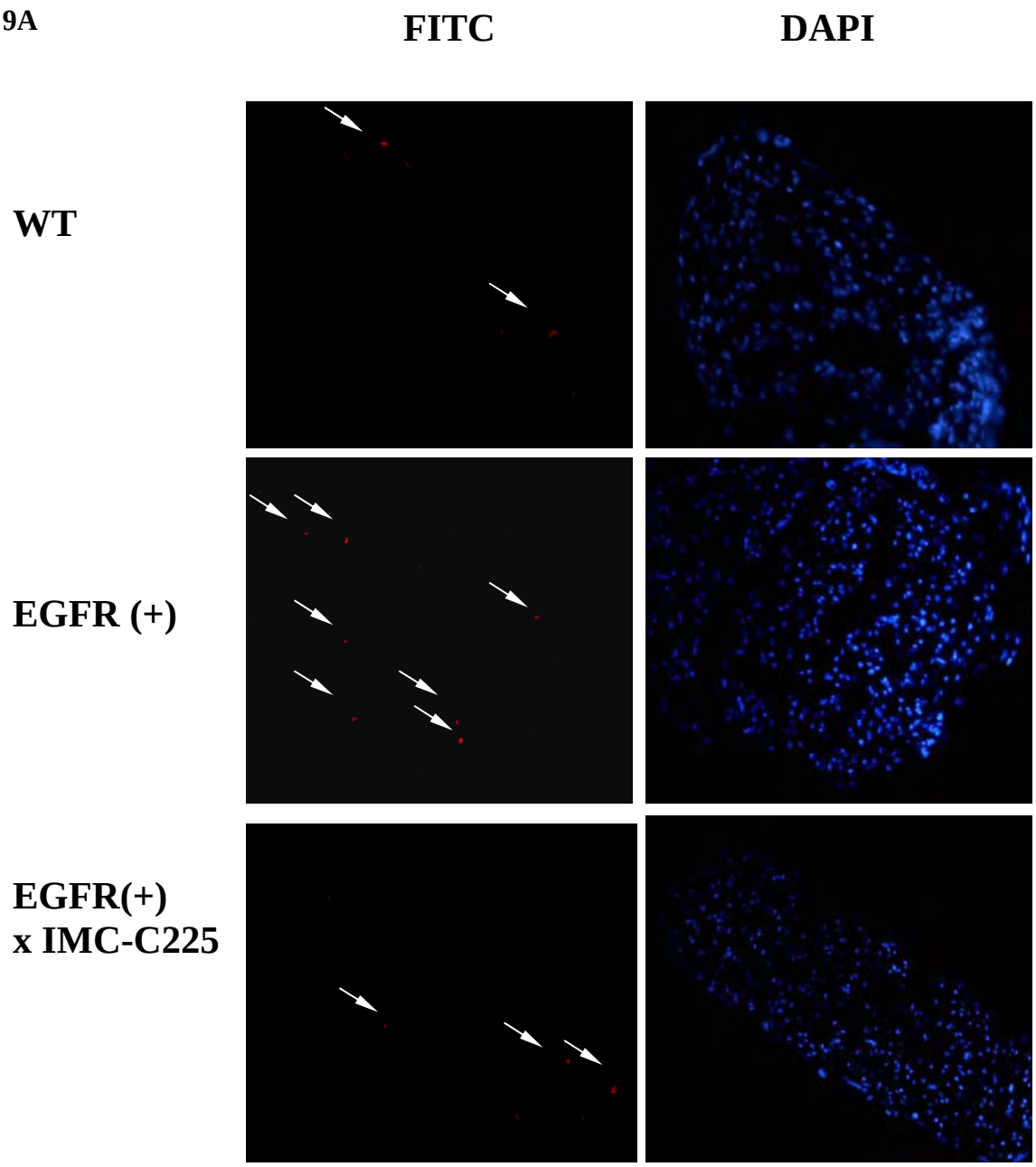

Fig 9B

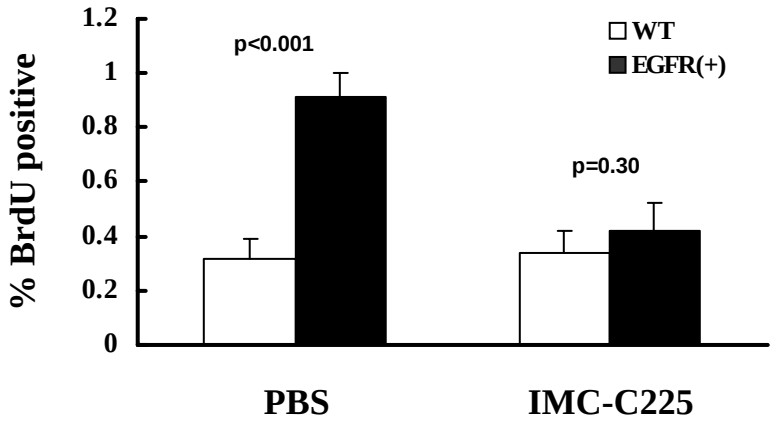

Fig 9C

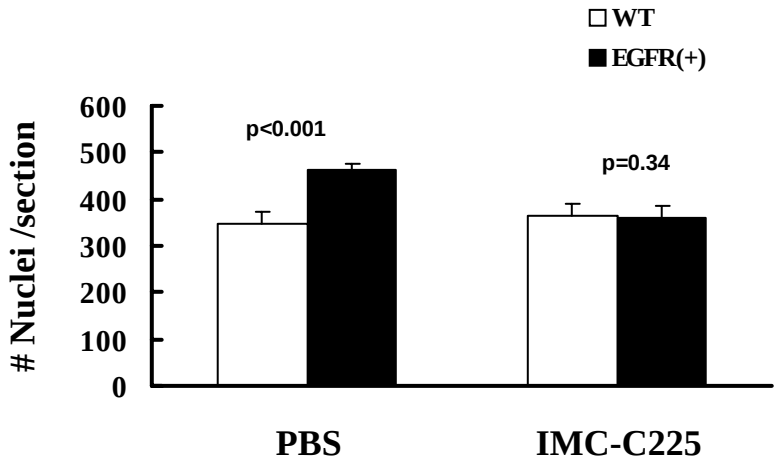

Fig. 9. IMC-C225 inhibits Schwann cell proliferation. BrdU incorporation was performed as described in Material and methods. (A) Immunofluorescence of BrdU incorporation. The number of BrdU-labeled nuclei in the sciatic nerve of EGFR(+) mice (middle) was more than 3 fold higher than in wild type mice (top). After exposure to IMC-C225 for 2 weeks immediately after birth, BrdU positive cell number and sciatic nerve nuclei number also increased significantly ($p<0.01$, $n=4$, Fig 9C). After IMC-C225

treatment, BrdU-labeled nuclei nerve in transgenic mice decreased to wild type level (p=0.30, n=4, Fig 9B). Nuclei number also decreased after IMC-225 treatment, so that there was no longer a significant difference comparing to the wild type level (p=0.34, n=4). Taking into account the inhibition of hEGFR auto phosphorylation by IMC-C225, we conclude that IMC-C225 blocks hEGFR-driven Schwann cell proliferation in this mouse model.

Thermal sensory decrease in EGFR mouse

Small caliber axons ensheathed by non-myelin forming Schwann cells convey most sensory information. The abnormalities in unmyelinated fiber bundles and non-myelinated Schwann cells in CNPase-EGFR transgenic mouse raised the possibility that the sensation was decreased or lost in this mouse model. We used a test of heat sensitivity to assess this possibility. Mice were placed on a 50°C plate and time to paw lift measured. Significantly decreased heat sensitivity was found in 3 month old transgenic mice as compared to wild type littermates (p=0.009, n=7).

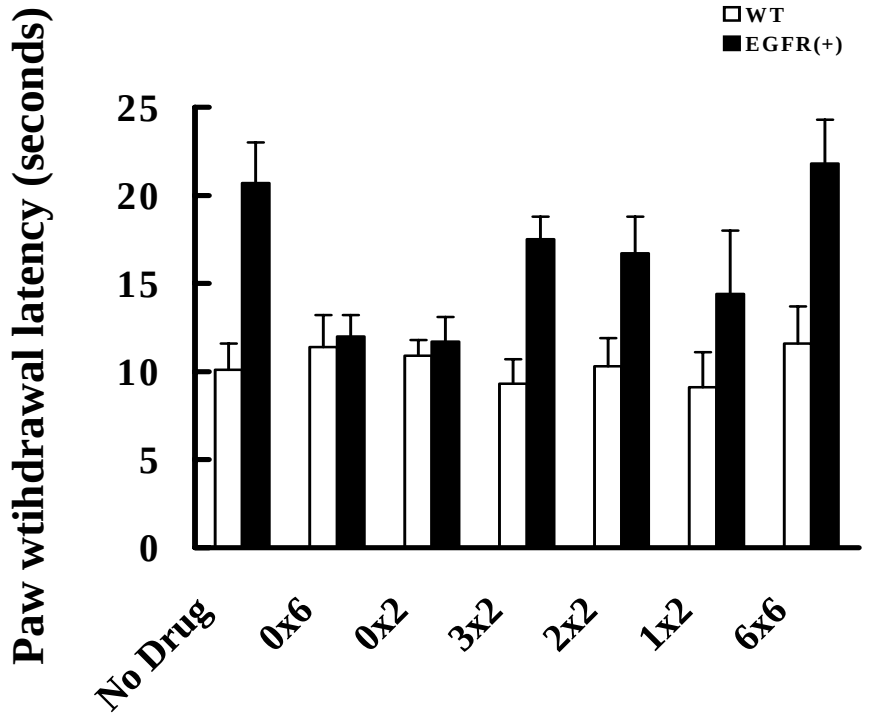

Fig. 10. Thermal sensory decrease in EGFR(+) mouse. Mice (hEGFR ot wild type) were treated with IMC-C225 or PBS at different time and were tested for heat sensitivity at 3 month old of age. Paw withdrawal latency was significantly decreased in hEGFR transgenic mice (black bar) comparing to wild type countparts (white bar) (p=0.009, n=7). In

early IMC-C225 treatment groups, either treated for 2 weeks or 6 weeks, there were no thermal sensory change in transgenic mice (p= 0.32, n=6 for 2 weeks group, p=0.36, n=5 for 0-6 weeks group). Heat sensitivity loss did happen in later drug treatment group (p=0.01, n=6). In groups that mice were exposured to IMC-C225 from one to three weeks, the thermal sensitivity were partially changed. Thus hot plate testing can be used as a measure of nerve disruption in the hEGFR transgenic mice.

Based on these results, we tested the thermal sensitivity in IMC-C225 treated transgenic or wild type mice. The dosing schedule is shown in figure 7. Strikingly, IMC-C225 treatment of mice for 2 weeks or 6 weeks beginning at birth, restored thermal sensation to wild type levels (p= 0.32, n=6 for 2 weeks group, p=0.36, n=5 for 0-6 weeks group) (Fig. 10). However, treatment beginning at 6 weeks of age was ineffective in reversing the hEGFR-driven phenotype (p=0.01, n=6). Interestingly, if mice were treated from one to three weeks, the thermal sensitivity was partially reversed. The data implied that early treatment of IMC-C225 reverses the transgenic mice phenotype, while later treatment has little or no effect.

Late drug treatment has no effect on reversing hEGFR nerve histology phenotype

To confirm these results we carried out detailed histology on nerves from the cohort of wild type and mutant mice. 6 week old hEGFR or wild type mice were treated with IMC-C225 twice a week for 2 weeks. Saphenous nerve sections from mice 3 months of age were chosen for analysis of nerve area, re highly disrupted in this model (Ling et al., 2005).

As shown in Fig 11, there remained significant differences between transgenic mice and wild type mice in nerve area ($p<0.001$, n=6), nerve nuclei number ($p<0.001$, n=6) and mast cell number ($p<0.001$, n=6) (Fig

11 A-C). This showed that brief late treatment caused no effects on reversing the nerve function and hEGFR mouse phenotype.

Fig 11A

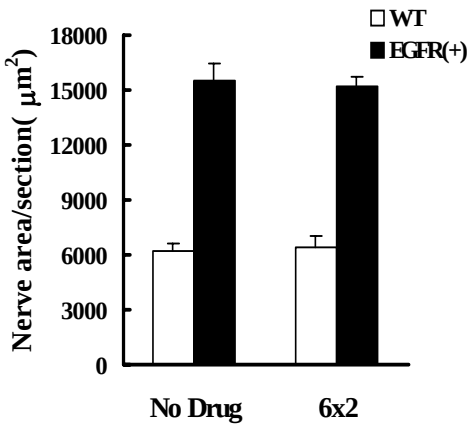

11C

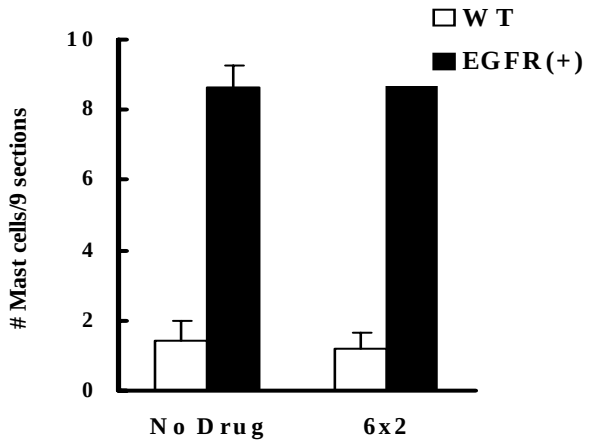

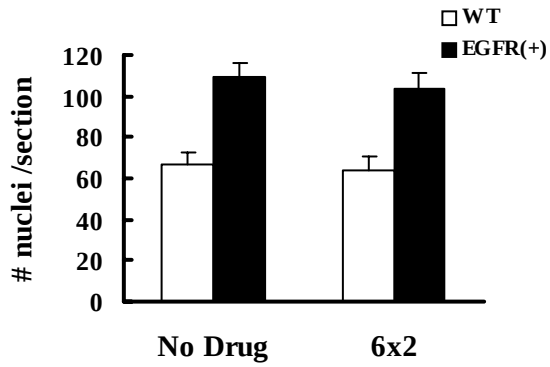

11B.

Fig. 11. Later drug treatment has no effect on revering phenotype. Saphenous nerve of 3 month old mice treated with or without IMC-C225 were tested for nerve area, nuclei counts and mast cell number. (A) Nerve area, there was a significant difference between transgenic mice (black bar) and wild type mice (white bar) in nerve area ($p<0.001$, n=6). (B) Nuclei counting: significant difference between transgenic mice (black bar) and wild type mice (white bar) was found in nuclei counts ($p<0.001$, n=6). (C) Mast cell number. There was a significant difference between transgenic mice (black bar) and wild type mice (white bar) in mast cell number ($p<0.001$, n=6).

Early treatment reverses the mouse nerve histology phenotype

hEGFR and wild type mice were injected with IMC-C225 immediately after birth and twice weekly for 2 or 6 weeks . Saphenous nerve sections from 3 month old mice were tested for nerve area, nuclei counts, mast cell number and collagen deposition.

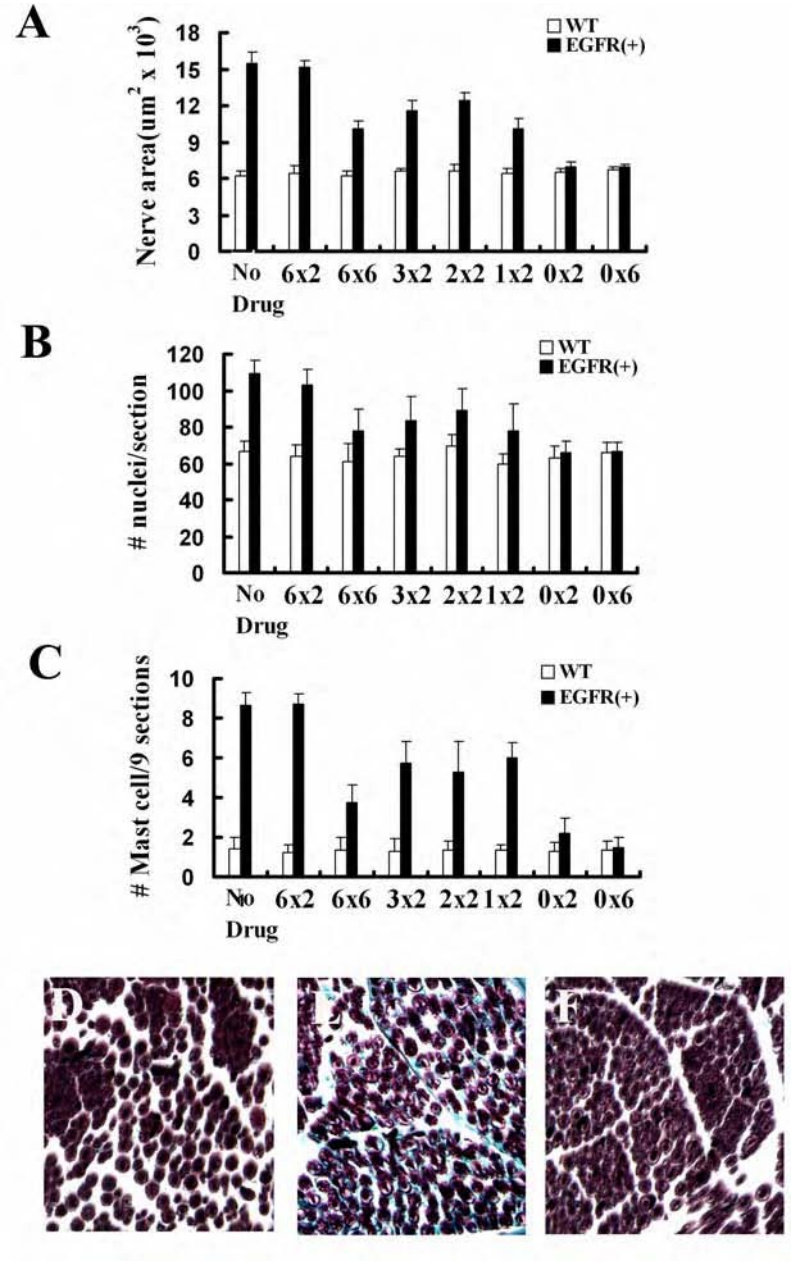

Fig. 12 Early treatment reverses the mouse phenotype. Saphenous nerve of 3 months old mice treated with or without IMC-C225 were tested for nerve area, nuclei counts and mast cell number. (A) Nerve area, there was no significant difference in transgenic mice (black bar) and wild type mice (white bar) in nerve area (p=0.36, n=5 for 0-2 weeks group, p=0.32, n=6 for 0-6 weeks group) (B) Nuclei counting: no significant difference was found between transgenic mice (black bar) and wide type mice (white bar) in nuclei counting (p=0.10, n=5 for 0-2 weeks group, p=0.28, n=6 for 0-6 weeks group). (C) Mast cell number: no significant difference was found between transgenic mice (black bar) and wide type mice (white bar) in mast cell counting (p=0.36, n=5 for 0-2 weeks group, p=0.32, n=6 for 0-6 week group) decreased to wild type level (low). (B) Quantification of BrdU positive percent in IMC-C225 or PBS treated hEGFR (black bar) or wild type mice (white bar). There was significant difference in %BrdU positive in PBS treatment group ($p<0.001$, n=4). No

significant difference was found in IMC-C225 treatment group. ($p=0.30$, $n=4$). (C). Quantification of sciatic nuclei number in IMC-C225 or PBS treated hEGFR (black bar) or wild type mice (white bar). There was significant difference in nuclei number in PBS treatment group ($p<0.001$, $n=4$). Nuclei number decreased after IMC-225 treatment and there was no significant difference comparing to the wild type level ($p=0.34$, $n=4$).

Early exposure to IMC-225 reverses defects in axon-glial interactions

Groups of small unmyelinated axons cluster within single non-myelin forming Schwann cells, while myelinated Schwann cells show 1:1 interaction with large axons. These intimate interactions between axons and Schwann cells can be monitored by transmission electron microscopy. We therefore analyzed saphenous nerves of mutant mice before and after drug treatment using this method. As shown in Fig. 13a, 3 month old hEGFR mouse nerves contain disrupted small axon fiber bundles. NMSCs display long aberrant process which wrap one or two, or no, small axons. After being treated with IMC-C225 for 2 or 6 weeks immediately after birth, the hEGFR sapphenous nerve Schwann cells were morphologically indistinguishable by electron microscopy from their wild-type counterparts at 3 months of age. In contrast, mice treated beginning at 6 weeks old contained nerves ultrastructure characteristic of untreated hEGFR mice. These EM results provide further evidence that early IMC-C225 treatment prevents the peripheral nerve dysfunction driven by hEGFR expression in Schwann cells, while later treatment is ineffective.

Fig. 13. Early exposure to Cetuximab restores axon-glial interactions. (A-D). Electron micrographs of saphenous nerves from 3 month old animals. (A). Wild type nerves showed characteristic groups of small unmyelinated axons clustered within single non-myelin forming Schwann cells. (B). Untreated CNPASE-HEGFR nerves were disrupted; non-myelinating Schwann cells rarely wrap multiple axons. (C-D). CNPase-hEGFR nerves treated with Cetuximab beginning at birth for 2 weeks (C) or 6 weeks (D) showed wild type levels of nerve organization; non-myelinating Schwann cells were able to wrap multiple small axons. (For A-D, micrographs shown at 9375X). (E). Quantification of percentage of grouped axons in nerves from wild type (WT), untreated CNPase-hEGFR (EGFR+), CNPase-hEGFR mice treated from birth for two weeks (0x2), birth to six weeks (0x6),six to eight weeks (6x2) or six to tweleve weeks (6x6) of age. Small axons are considered grouped if three or more are wrapped by a single non-myelinating Schwann cell. Untreated CNPase-

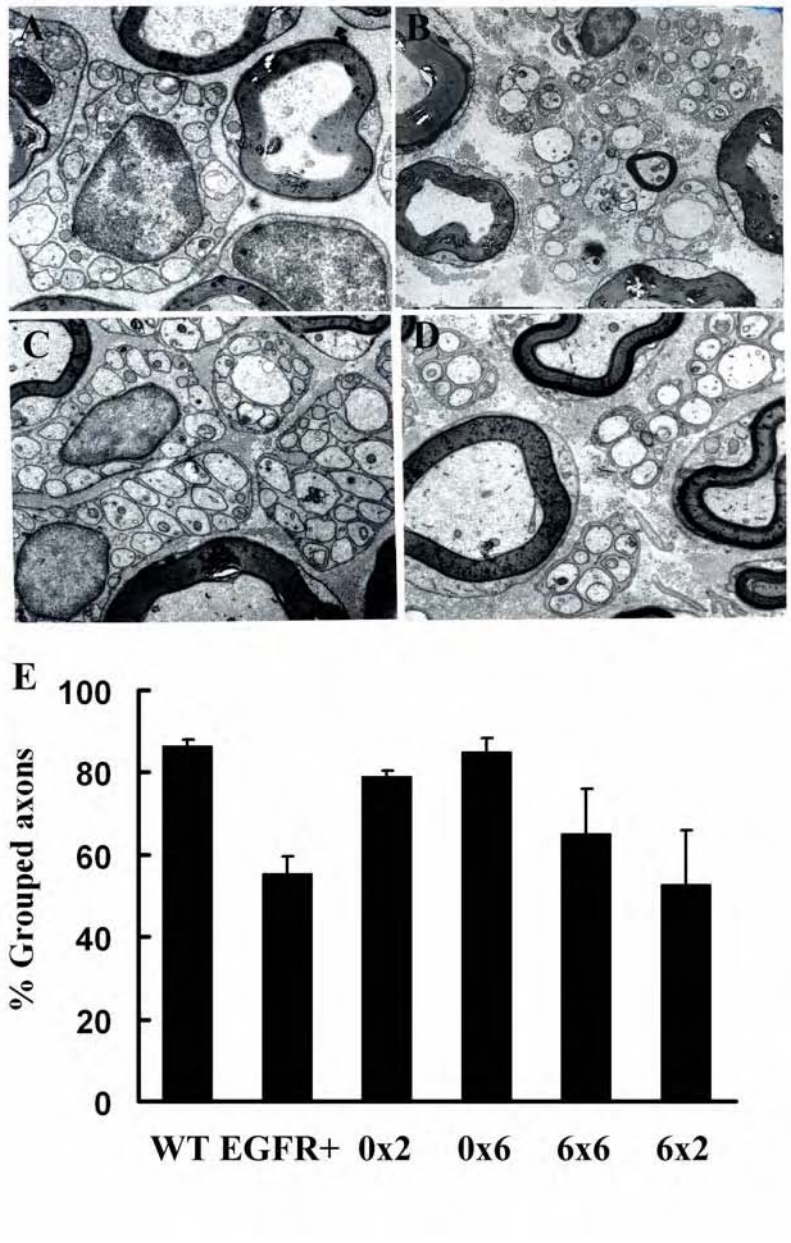

hEGFR nerves were significantly more disrupted than wild type. CNPase-hEGFR nerves treated with Cetuximab beginning at birth did not differ significantly from wild type.

***Nf1*+/- mouse nerves contain a population of EGFR$^+$/p75$^+$ cells**

The results indicate that an EGFR-expressing cell present around birth might account for much of the abnormality in this EGFR-expressing model. This raised the possibility that an EGFR+ cell might also exist in Nf1 model system. If *Nf1* predisposes to EGFR expression within the perinatal period, it should be possible to detect EGFR+ cells in *Nf1* mutant peripheral nerve. To test this, we dissociated cells from P0-P1 mouse sciatic nerves, and stained cells with antibodies recognizing EGFR and the Schwann cell marker p75 in 3 experiments using 2-4 individual pups/genotype per group. We identified EGFR/p75 double positive cells among *Nf1*+/- mouse Schwann cells (Fig. 14B) but very low in wild type cells (Fig. 14A). Among 10,000 cells counted in each genotype, only 2 were EGFR+ and p75+ positive from wild type nerves, these did not show punctuate EGFR staining characteristic of cells in mutant nerves. Quantification revealed >250-fold increase in double positive cells in *Nf1*+/- mouse nerve cell

preparations, compared to cells from wild type mice (Fig. 14C).

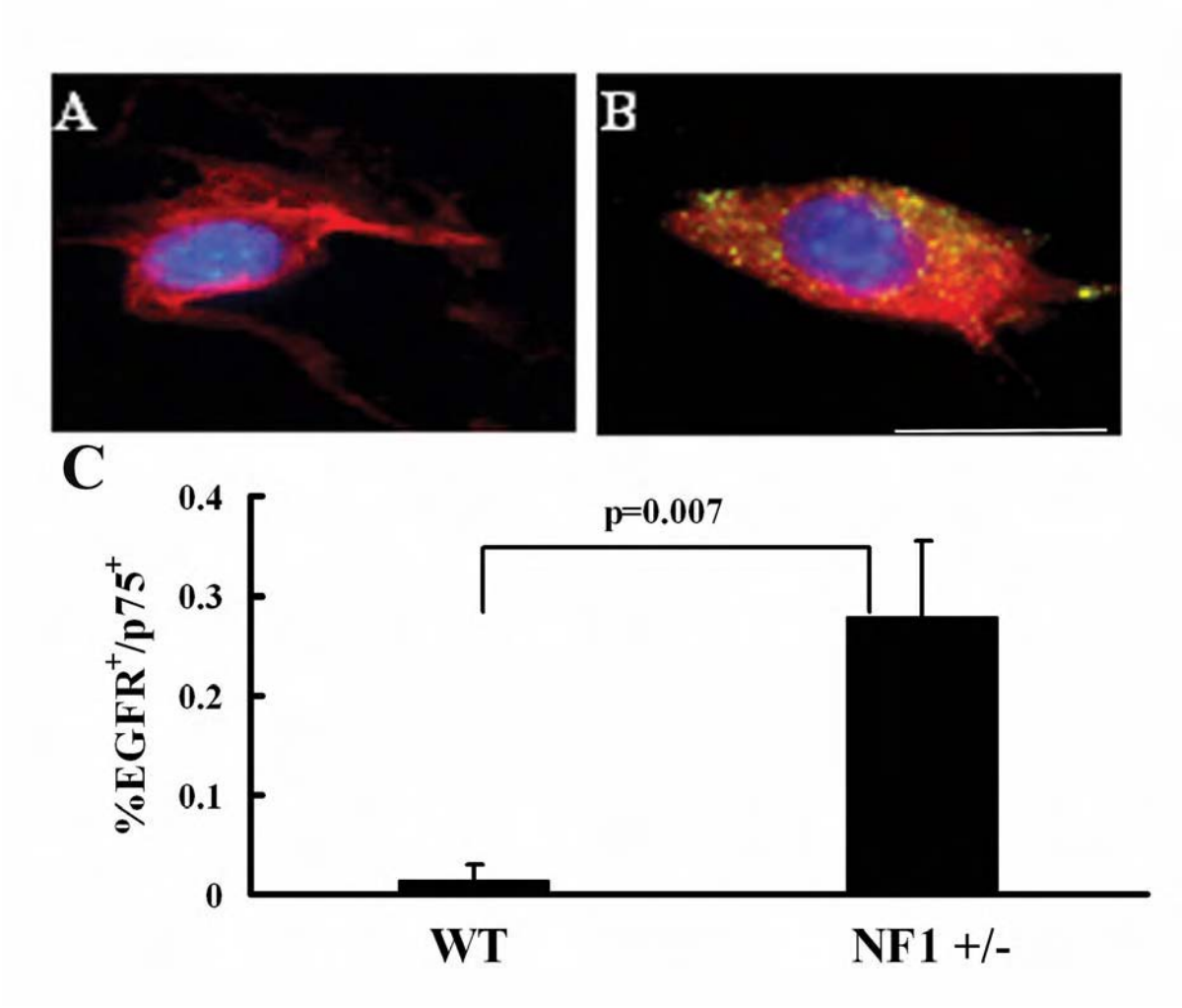

Fig. 14. *Nf1*+/- mouse nerves contain EGFR$^+$/p75$^+$ cells. (A-B). Schwann cells were dissociated from P0-P1 mouse sciatic nerves and stained with anti-EGFR (green) and anti-p75 (red). (A). Representative wild type cell is p75+. (B). *Nf1*+/- cells showing double staining for EGFR and p75. Bar = 10um. (C). Graph shows quantification of percentage of EGFR$^+$/p75$^+$ cells in wild type (WT) and *Nf1*+/- nerves. The difference between *Nf1*+/-and wild type nerve was significant (p=0.006; *Nf1*+/- n=9, WT: n=6).

EXPERIMENTAL PRECEDURE

Animals

CNPase-hEGFR transgenic mice were genotyped by PCR as described (Ling et al, submitted). Mice were on the FVBN strain (N= 6). Mice were housed in a temperature- and humidity-controlled viaticum that was kept on a 12-h dark-light cycle with free access to food and water. The animal care and use committee of the University of Cincinnati approved all animal use.

Drug treatment design

Cetuximab (MC-C225, ImClone, New York, NY), which blocks human but not rodent EGFR function, was injected intraperitoneally (i.p.) twice weekly at a dose of 1mg/25g, the injection dose and volume was adjusted according to the mice weight. Control group was injected with same volume of PBS. 12-16 mice were in each group. Mice were treated with IMC-C225 for 0-2 weeks, 1-3 weeks, 2-4 weeks, 3-5 weeks, birth–6 weeks, 6-8 weeks or 6-12 weeks of age. Mice were sacrificed at 2 weeks old or at 3 months of age. The dose and time schedule diagram is shown in Fig.1.

Hot plate test (nerve sensory test)

Hot plate procedures were reviewed and approved by the animal care and use committee of University of Cincinnati before the study was initiated and the study was conducted in compliance with the American Association for Accreditation of Laboratory Animal Care and the ethical guidelines of the International Association for the study of pain.

The hotplate test was performed in a quiet environment during the day using an electronically controlled hotplate analgesia meter (Columbus Instruments, Columbus, OH) heated to 50°C (±0.1°C). Mice were housed in a separated room and conditioned for one week before the test. The time it took the animals to begin licking their forelegs or hind paws was recorded. The cut-off time was set at 30 s to minimize tissue damage (33, 34).

Immunofluorescence

After IMC-C225 treatments for 2 weeks, mice were fixed by intracardial (i.c.) perfusion with 4% paraformaldehyde in PBS. Sciatic nerves were dissected, cryoprotected and cut in 10 μm sections for immunofluorescence staining as described before (35). Briefly, section slides were fixed in 4% (w/v) paraformaldehyde at room temperature (22–25 °C) for 10 minutes. After blocking with PBS containing 10% (w/v) rabbit serum for 1 h at room temperature, individual sections were washed 3 times with PBS and incubated with p-EGFR antibody (Santa Cruz Biotechnology, Inc., Santa Cruz, CA. 1:250) overnight at 4°C followed by incubation with Alex 488 rabbit anti-goat IgG and propidum iodine for 1 h at room temperature. Slides were air dried, cover-slipped and viewed with a laser confocal microscope equipped with a digital imaging system.

Cell proliferation (BrdU incorporation)

Mice were injected (i.p.) with a BrdU solution in PBS (50 mg BrdU per kg of body weight) for 3 times at 2hrs intervals (total 6 hrs) before intracardial perfusion. Sciatic nerves were dissected, paraffin-embeded, cut into 10-μm sections and processed for BrdU immunostaining. Briefly, sections were deparaffined in xylenes, fixed in 100%, 90%, 70% ethanol sequentially, washed 3× in PBS, treated with 2M HCl for 30 min at 37 °C, washed again 3× in PBS, and blocked in PBS containing 0.15% triton X-100 and 5% donkey serum. Sections were then incubated with a rat anti-BrdU antibody (Zymed Labortories Inc, South San Francisco, California, 1:200) overnight at 4 °C. The detection was carried out using TRITC-conjugated secondary antibody. Nuclei were stained with DAPI (Sigma Chemical Corp, St Louis, MO) for 5 min. The BrdU-labeled cells and the number of DAPI nuclei were counted in at least three cross sections made through each sciatic nerve. Data are presented as the average numbers of BrdU-labeled cells per section.

Electron Microscopy

Mice were perfused (i.c.) with Karnovsky's fixation solution (3% paraformaldehyde + 3% glutaraldehyde in 0.1M PB, pH 7.4-7.6). Saphenous nerves were dissected and immersed in the same fixative solution

overnight at 4°C, and then in 0.1M sodium cacodylate buffer (pH 7.2) for 2-3 hrs. Nerves were washed in PBS, post fixed with 2% osmium tetroxide and 0.6% potassium ferrocyanide and embedded in Embed plastic. Semi-thin sections (1 μm) were stained with toluidine blue and examined by light microscopy. Thin section photographs were obtained using a JEOL 100CX electron microscope.

Quantification of saphenous nerve area, nuclei counting and mast cell number

Mice were perfused (i.c.) with 4% paraformaldehyde made with 0.1M PBS. Sciatic and saphenous nerves were dissected and immersed in the same fixative solution overnight at 4 °C and then immersed in 70% ethanol and paraffin embedded. Every fifth cross sections (6 μm) were cut and mounted. DAPI, toluidine blue and Gamori's trichrome stainings were performed for nuclei counting, mast cell counting and collagen deposition respectively. MetaMorph image analysis software (Universal imagine corporation, Downingtown, PA) was used to quantify the nerve area of toluidine blue stained sections. Three cross sections made through each nerve were analyzed. Data are presented as the average numbers of per section.

Real time PCR

Messenger RNA was extracted from wild-type, $EGFR^{+}$, and IMC-C225-treated $EGFR^{+}$ mouse sciatic nerve using the Micro-FastTrack^{TM} kit for isolation of mRNA from small samples (Invitrogen, Carlsbad, CA). The mRNA was reverse transcribed using the Superscript Preamplification System (Gibco-Invitrogen, CA). Superscript II reverse transcriptase was used in the reaction, as per manufacturer's protocol. Duplicate samples lacking reverse transcriptase were conducted to control for genomic DNA contamination. Mouse GAPDH primers (sense, 5'-ACCCAGAAGACTGTGGATGG and antisense, 5'-GGAGACAACCTGGTCCTCAG. Expected product size, 300 bp) were included in each reaction as a positive control for cDNA.

For quantitative real-time PCR experiments, cDNA was used (as generated above), as were the following primers: Brain derived neurotrophic factor (BDNF; sense, 5'-TGGCTGCACTTTTGAGCAC and

antisense, 5'-GCAGTCTTTTTATCTGCCGC. Expected product size, 292 bp), Monocyte Chemoattractant Protein 1 (MCP-1; sense, 5'-AGCACCAGCCAACTCTCACT and antisense, 5'-CGTTAACTGCATCTGGCTGA. Expected product size, 136 bp), Stem Cell Factor (SCF; sense, 5'-CAGTCTTCAGGAGTGAGCCC and antisense, 5'- CAAAGATGCTCCCAAACGCT. Expected product size, 254bp), Transforming Growth Factor β1 (TGF-β1; sense, 5'-TGAGTGGCTGTCTTTTGACG and antisense, 5'- TCTCTGTGGAGCTGAAGCAA. Expected product size, 293bp). Triplicate reactions were performed in an ABI Prism 5700 Sequence Detection System Cycler according to the manufacturer's instructions. Briefly, 1 µl cDNA or water control was placed into a 50-µl reaction volume containing 25 µl SYBR Green Master Mix (2x concentration, Applied Biosystems) and volumes of primers that ranged between 2 µl and 9 µl, depending on the optimal conditions for each primer set. The remaining volume was comprised of water. The thermal cycling conditions comprised an initial equilibration step at 60˚C (2 min), a denaturation step at 95˚C (10 min), followed by 40 cycles of 95˚C (15s), 60˚C (1 min). Cycle threshold (C_t) values were obtained from the point during amplification at which the fluorescent intensity was in the geometric phase, as determined by PE Biosystems analysis software. All PCR products were analyzed on a 2% agarose gel. The ΔC_t values were determined for wt, $EGFR^+$, and IMC-C225-treated $EGFR^+$ nerve and relative ligand expression was calibrated to GAPDH expression (primers as above). Fold change of cytokines in $EGFR^+$ and IMC-C225-treated $EGFR^+$ nerve compared to wild type levels were calculated using the established equation[1]: $2^{-\Delta\Delta Ct}$, where C_t is the cycle number at the chosen amplification threshold, $\Delta C_t = C_{t(cytokine)} - C_{t(GAPDH)}$, and $\Delta\Delta C_t = \Delta C_{t(-/-)} - \Delta C_{t(+/+)}$.

Analysis of EGFR+p75+ cells from perinatal nerves

We dissected sciatic nerves from individual mouse P0 or P1 pups and dissociated nerves in L-15 medium containing 1.25U/mL Dispase Π (Roche, Indianapolis, IN), 156U/mL Collagens type I (Worthington, Lakewood, NJ) for 30 minutes. We collected cells by centrifugation and plated them onto

poly-L-lysine and laminin coated 8 well lab-Tek chamber slides in DMEM medium containing 10% FBS and 1% Pen/Strip. Medium was changed the next day to remove debris. Cells were fixed 24h later with 4% paraformaldehyde, then double stained with goat anti-EGFR (Santa Cruz, CA, SC-03-G, 1:20) and rabbit anti-p75 (Chemicon, Temecula, CA, AB1554, 1:200) antibodies, followed by secondary antibodies Donkey anti-goat Alexa-488 (for EGFR, Molecular probes, Eugene, OR, 1;2000) and Mouse anti-rabbit TRITC (Molecular probes, OR, 1:200). Nuclei were counter-stained with DAPI. MPNST cell line 8814 (EGFR positive) and Goat IgG were used as positive and negative controls. Three independent experiments were performed with a total number of 9 *Nf1*+/- and 6 wild-type pups. For each Lab-Tek well, 10 random fields were chosen for cell counting. The genotype was blind during counting. We used 2-tailed Student's *t*-test for data analysis.

Data analysis

For all quantitative analysis, at least three sections from each nerve were analyzed. Statistical significance was determined by Student's *t*-test. $P < 0.05$ was considered significant.

Task 1c, In Progress: Evaluate effects of an anti-fibrotic drug, pirfenidone.

Our move to the Children's Hospital Research Foundation allowed us to obtain pirfenidone. We decided to wait to obtain a more robust model to do this experiment. To this end, we bred the CNPase-hEGFR mouse to obtain homozygotes for analysis and treatment. We screened 80 EGFR offspring of EGFR/+ x EGFR/+ mice, by breeding to wild type mice to confirm homozygosity. We obtained the anticipated 20 EGFR/EGFR homozygotes. As shown in Figure 15, nerves of mutant mice were enlarged, and 25% developed tumors. Electron microscopic evaluation of the peripheral nerves of the mice shows more profound disruption of axon-glial interactions than heterozygotes, which is being quantified.

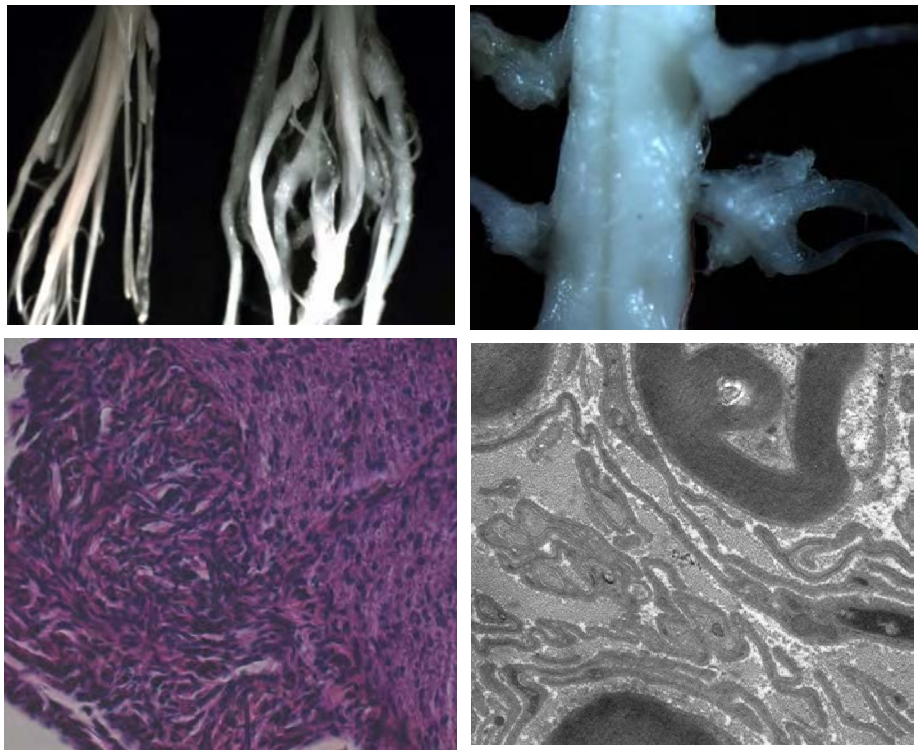

Figure 15. Characterization of EGFR/EGFR nerves and tumor. Upper left, dissection of cauda equina of wild type (left) and hypertrophied EGFR/EGFR mice (right). Upper right, right side of spinal cord shows putative tumors assicoated with DRG in an EGFR/EGFR mouse. Lower left, histology of one of the masses. Lower right, electron micrograph of EGFR/EGFR nerve at 3 months of age.

We aged 15 mice to 15 months; the mice carrying two EGFR transgenic alleles show reduced survival as compared to the heterozygotes.

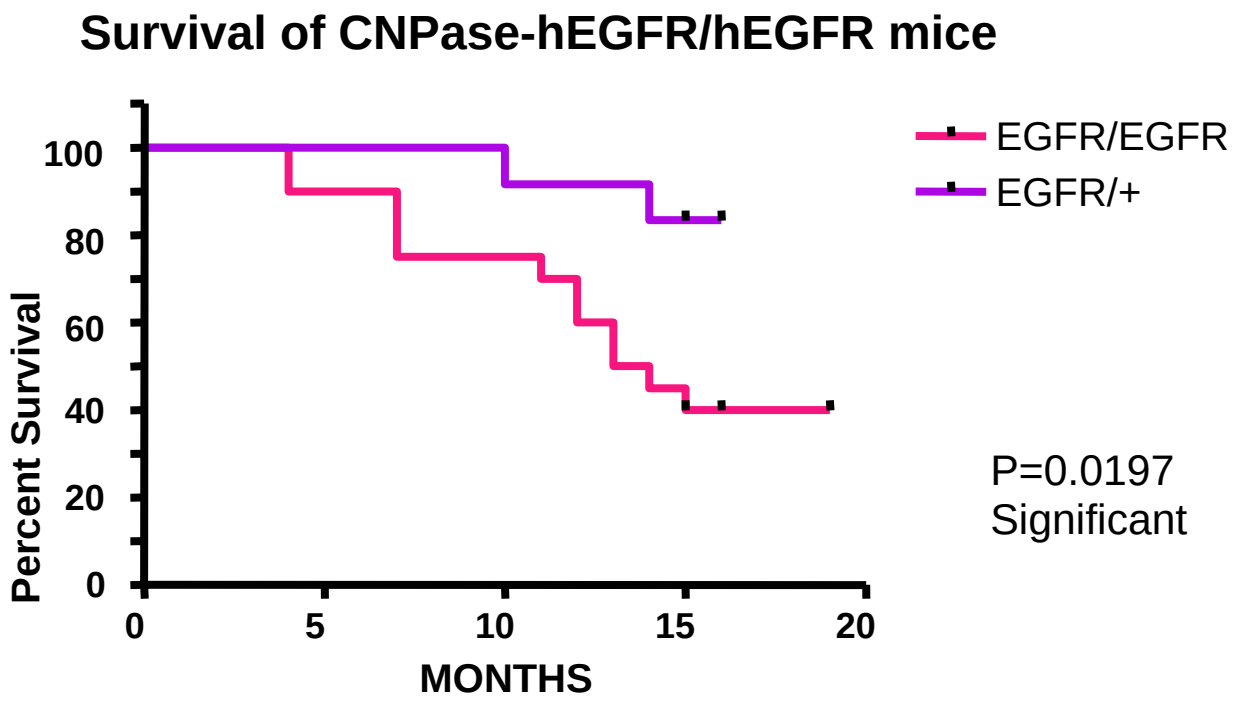

Figure 16. Kaplan Meyer analysis of EGFR/EGFR homozygous mice. EGFR/EGFR n=20. EGFR/+ n = 12 mice. All mice are on the FVBN/C57Bl\6 background.

Pirfenidone experiment

16 EGFR/EGFR mice, 5.5 months, mice were randomly divided into two groups with ad libitum access to water with (Group I) or without (Group II) 0.5% (w/w) peifenidone. The water was changed once a week. All mice were sacrificed at 7.5 months. 3 of 8 mouse sciatic nerves from each group were dissected for collagen quantification. The other 5 mice were perfused (intracardially) with 4% paraformaldehyde in 0.1 mol/L PBS. We dissected sciatic and saphenous nerves and immersed them in

the same fixative solution overnight at 4°C before paraffin-embedding. Every fifth cross-section (6 µm) has been cut and mounted. Three cross sections through each nerve will be analyzed. DAPI, toluidine blue, and Gomori's trichrome stainings will be performed for nuclei counting, mast cell counting, and collagen deposition, respectively. MetaMorph image analysis software (Universal Imagine Corp., Downingtown, PA) will be used to quantify the nerve area of toluidine blue-stained saphenous sections and statistical significance determined by two-tailed Student's *t*-test or ANOVA as appropriate.

Task 2: Study signaling defects in EGFR-expressing mouse.

Task 2a. Mate to 12V-H-Ras over-expressing mice ***and*** *to mice hemizygous for Nf1 mutation*.

The experiment 12V-Ras experiment does not make sense any longer, as there was no effect of mating to the *Nf1* mice as shown above, in Figures 2 and 5.

Task 2b. Define abnormalities in nerves of mice overexpressing EGFR and hemizygous for Nf1 mutation.

The *Nf1;EGFR* nerves do not look different from nerves from *Nf1* mutants only (data not shown).

Task 2c. Biochemistry of signaling on nerves from mice, by analysis of Ras-GTP, phospho-AKT and phospho-ERK (Year 3)

Task 2e. Evaluate the role of EGFR in MPNSTs tumorigenesis.

To test if EGFR plays an important role in mouse MPNST tumorigenesis, we originally planned to evaluate anti-EGFR therapeutics on xenografts of MPNST cell lines, with Jeffrey DeClue at NCI. However, Dr. DeClue has left research. We accomplished our goal of testing if loss of EGFR is important in an *Nf1*-driven model system of sarcoma in another way. Last year we crossed the $Nf1^{+/-}; p53^{+/-}$ Cis mouse (NPCis; obtained from Dr. Kristine Vogel) with EGFR $^{wa\text{-}2}$/+ mice, which lack 90% of EGFR activity from one allele due to a hypomorphic mutation.

$Nf1^{+/-}$; $p53^{+/-}$ mice carry the *Nf1* and *p53* mutations in cis on mouse chromosome 11 (Vogel et al., 1999). Mice had been backcrossed six generations onto the C57Bl\6 background at the time of the

experiment. The tumor spectrum on this background has been described (Reilly et al., 2000). We obtained C57BL/6J $^{wa-2}$/+mice from the Jackson Laboratory. We established the lines of mice segregating *Nf1*$^{+/-}$; *p*53$^{+/-}$; Egfr^{wa2}/+, *Nf1*$^{+/-}$; *p*53$^{+/-}$; +/+, *Nf1*$^{+/-}$; *p*53$^{+/-}$;Egfr^{wa-2} /+ and *Nf1*$^{+/-}$; *p*53$^{+/-}$;+/+ by crossing *Nf1*$^{+/-}$; *p*53$^{+/-}$ with Egfr^{wa2} /+carriers. Mice were housed in a temperature- and humidity-controlled viaticum that was kept on a 12-h dark-light cycle with free access to food and water. The animal care and use committees of the University of Cincinnati and the Cincinnati Children's Hospital Research Foundation approved all animal use. We genotyped *Nf*1 and p53 alleles as reported (Vogel et al., 1999). We genotyped Egfr^{wa-2} by PCR amplifying a 170-bp region (primers: 5′-CCCAGAAAGGGATATGCG-3′ and 5′-GCAACCGTAGGGCATGAG-3′) and digesting with FokI to produce an uncut 170-bp or cut 75- and 95-bp fragments diagnostic for wild-type (wt) *Egfr* and *Egfr*^{wa2} alleles, respectively (Luetteke et al., 1994).

We have now finished this experiment. At 26 weeks, we published the data. The *Nf1*$^{+/-}$; *p*53$^{+/-}$ mice developed tumors at as early as 15 weeks and 8 (50%) died at 23 weeks, while only 1 of 17 (5.9 %) *Nf1*$^{+/-}$; *p*53$^{+/-}$;EGFR^{wa-2}/+ developed spindle cell tumor sarcoma at 18 weeks and required sacrifice. As for the other 16 mice, they have all survived beyond 26 weeks and none have developed visible tumors at the time of publication. Thus a deficiency of EGFR alters *Nf1*$^{+/-}$; *p*53$^{+/-}$ mouse mortality. We found that introduction of EGFR mutation decreases tumor formation time and mortality rate significantly ($p<0.05$) in the *Nf1*$^{+/-}$; *p*53$^{+/-}$ model system. We have now continued to follow *Nf1;p53;wa-2* triple heterozygotes until 42 weeks. As shown in Fig. 17, decreased EGFR tyrosine kinase activity delayed but did not stop tumor formation.

Figure 17. Survival of *Nf1*$^{+/-}$; *p*53$^{+/-}$ mice as compared to *Nf1*$^{+/-}$; *p*53$^{+/-}$;EGFR^{wa-2}/+ mice.

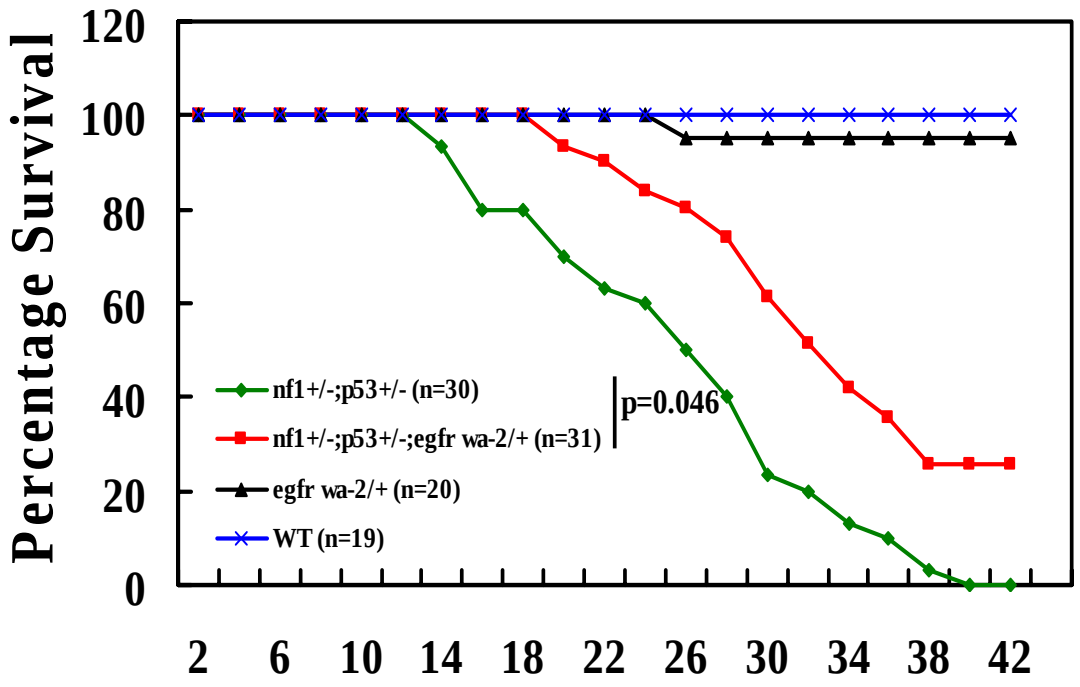

KEY RESEARCH ACCOMPLISHMENTS

- An ongoing debate in neurofibromatosis research is whether *NF1* mutant Schwann cells need co-operation from mutant, surrounding cells to drive neurofibroma formation. Our data shows that EGFR expression in Schwann cells drives mast cell accumulation and fibrosis typical of human neurofibromas, without a mutant environment.
- In contrast to EGFR-mutant brain tumor models, in the peripheral nerve a wild type *EGFR* allele drives tumorigenesis.
- The expression of wild type EGFR results in ensheathing, but not myelinating, Schwann cells losing contact with axons. This suggests that the specialized non-myelin forming Schwann cell may be an affected cell type in neurofibroma formation.
- The work defines a novel model of neurofibroma formation and reveals a function for EGFR activity independent or downstream of *Nf1* mutation.
- When mice were treated with Cetuximab beginning at birth, nerve hypertrophy, mast cell accumulation, collagen deposition and axon-glial interactions were normal at 3 months age. Hot plate sensory tests confirmed histology and electron microscopy data. These results suggest that application of therapies in young animals have the potential to block tumorigenesis by halting a crucial step in a cascade of events that leads to complex changes characteristic of neurofibroma formation.
- Identification of an EGFR expressing glial cell in *Nf1*+/- mice supports the hypothesis that this may be a target cell for expansion into neurofibromas.
- The great potential of EGFR-targeted therapies in the treatment of many types of cancer is prompting the continued development of specific agents targeted to the

extracellular ligand-binding domain, the intracellular tyrosine kinase domain, the ligand, or to synthesis of the EGFR.

- hEGFR mice have loss of thermal pain responsiveness. Diminished sensory function is consistent with the impaired axon-glial interactions in the model. Hotplate testing is a rapid and useful way to monitor therapeutic efficacy in the hEGFR transgenic mouse model system, and possibly other model systems of neurofibroma formation.
- The work suggests new and exciting directions in neurofibroma prevention and therapy. Our move to the Cincinnati Children's Hospital Research Foundation has allowed follow-up of results through collaboration with clinicians including John Perentesis, Brian Weiss and Elizabeth Schorry, with whom submitted an NF Center Grant proposal in Feb., 2006, which was favorably reviewed (although not funded), and which is being revised for a resubmission date of Feb., 2007.

REPORTABLE OUTCOMES:

Development of CNP-hEGFR transgenic mouse model. The mice were provided to Vittorio Gallo for analysis of CNS progenitors and to David Largaespada for identification of possible progression genes for neurofibroma and MPNST.

Development of *Nf1*$^{+/-}$; *p*53$^{+/-}$; EGFR$^{wa\text{-}2}$/+ mouse model system.

Development of EGFR/EGFR mice.

Papers:

Ling B, Wu J, Miller S, Monk K, Shamekh R, Rizvi T, Decourten-Myers G, Vogel K, DeClue J, Ratner N: Role for the epidermal growth factor receptor in neurofibromatosis-related peripheral nerve tumorigenesis. Cancer Cell 2005, 7:65-75

Monk, K., Wu, J., Langford, L. and **Ratner, N.** (2005) EGFR signaling in Neurofibromatosis Type 1. Proceedings of the Meeting on Glial Cell Functions in Health and Disease (Amsterdam, NL, May 17-21, 2005). (Invited review).

Aguirre, A., Rizvi, T.A., **Ratner, N**. and Gallo, V. (2005) Overexpression of the EGF receptor confers migratory properties to non-migratory postnatal neural progenitors, *J. Neurosci* 25(48):11092-106. Highlighted in "This Week in The Journal".

Wu, J., Crimmins, J., Monk, K., Williams, J., Fitzgerald, M., Tedesco, S. and **Ratner, N.** (2006) Perinatal EGFR blockade prevents peripheral nerve disruption in a model reminiscent of WHO Grade 1 neurofibroma, *Am. J. Pathol.,* 168(5), 1686-1696

Abstracts:

Aguirre,A. Rizvi,T.A, Ratner,N and Gallo,V. Overexpression of the epidermal growth factor receptor confers migratory properties to non-migratory postnatal neural progenitors. *2005 Abstract Viewer/Itinerary Planner*. Washington, DC: Society for Neuroscience, 2005.

Wu, J., Monk, K., Tedesco, S., & Ratner N. Brief EGFR blockade prevents peripheral nerve dysfunction in a mouse model of peripheral nerve tumorigenesis. Abstract # 5055. 96th American Association for Cancer Research Annual Meeting. Anaheim, CA. April 16-20, 2005.

Ling, B.C., Rizvi, T.A., Miller, S. J., DeClue, J.E. and Ratner, N (2002) Up-regulation of the EGF Receptor results in neurofibroma formation. J. Neurosurgery; presented by B. Ling, fellow,

SELECTED FOR PLATFORM TALK.

Monk, K.R., Meinhardt, B.A., Ling, B.C., Crimmins, J.T., Shamekh, R., Miller, S.J., Rizvi, T.A., Ratner, N. Mast cell contributions to nerve pathology in EGFR expressing mice. 2004. Mast Cells in Physiology, Host Defense and Disease: Beyond IgE. Keystone Meeting, Taos, NM. 76a. SELECTED FOR PLATFORM TALK.

Results were described by the PI in the following seminars:

2006 Amgen, Seattle, Washington

NNFF International Consortium Meeting Aspen, CO

International Society for Developmental Neuroscience, Banff, Canada

Ohio State University Cancer Center, Columbus, OH

Rutgers University, Newark, NJ (Women Student invited)

2005 Banbury Conference, Mouse Models of Neurofibromatosis, Cold Spring Harbor, NY

Center for Neuropharmacology and Neuroscience, Albany Medical College, Albany, NY

Symposium Speaker, Society for Neurochemistry, Madison WI

Symposium Speaker, Glial Biology in Health and Disease, Amsterdam

NNFF International Consortium Meeting, Aspen, CO

2004 NNFF International Consortium Meeting Aspen, CO

Experimental Hematology, Cincinnati Children's Hospital, Cincinnati, OH

2003 Dana Farber Cancer Institute Boston, MA

NNFF International Consortium Meeting Aspen, CO (presented by K. Monk, student)

Pathology of Mouse Peripheral Nerve Tumors, Boston, MA

2002 Dept. Biochemistry, University of Iowa, Ames, IA

ASCB National Association of Biology Teachers/Cincinnati, OH

NNFF International Consortium Meeting Aspen, CO

Primate Center, Oregon Health Sciences University, Portland, OR

Dept. Pharmacology, Washington University, St. Louis, MO.

Mouse Models Consortium, NF Satellite, Washington DC

Research opportunities:

Ben Ling received an ACS fellowship in support of his work on this project. Kelly Monk received a Ryan Graduate Fellowship in support of her work on this project and is now a postdoctoral fellow at Stanford. We supported Diana Schorry, an undergraduate from the University of Michigan, summers

2004 - 2006. In 2005, a rotating graduate student in our Developmental Biology Graduate Program and an undergraduate from Miami University worked on the project.

CONCLUSIONS

This study demonstrates the dramatic effect of expressing EGFR in mouse Schwann cells. Peripheral and cranial nerves in CNP-hEGFR mice exhibit diffuse changes that parallel the hallmarks of human cutaneous and plexiform neurofibromas. These include increased endoneurial collagen matrix, dissociation of Schwann cells from axons, Schwann cell hypercellularity, and mast cell accumulation. Changes were within the perineurium, as is common in plexiform neurofibromas. While previous studies showed that EGFR is expressed in MPNST cells and some neurofibroma Schwann cells (DeClue et al., 2000; Li et al., 2002), EGFR expression might have correlated with tumor formation rather than be a causative event. Strikingly, our data are consistent with a causative, and early, role for EGFR in progression to neurofibroma formation. EGFR overexpression is characteristic of and contributes to formation of many human cancers. Therapeutic reagents that target EGFR are in clinical trials (Yarden, 2001; Ranson et al., 2002) and, based on our data, could be considered as candidate therapeutics for NF1.

This study shows that EGFR expression in Schwann cells results in nerve hyperplasia with occasional neurofibroma formation. To develop neurofibromas at a higher rate, or malignancies, it may be necessary to cross these mice to strains with other mutations. Cre/lox mediated ablation of *Nf1* in Schwann cells resulted in nerve pathology similar to that observed here, but only when the mice also hemizygous for *Nf1* mutation (Zhu et al., 2002). Our model does not require mast cells and/or fibroblasts to be $Nf1^{+/-}$, as crossing hEGFR to $Nf1^{+/-}$ mice did not increase nerve size or mast cell number. The similar phenotype of hEGFR nerves to nerves in mice, and humans, with loss of function mutation at *Nf1* (Cichowski et al., 1999; Zhu et al., 2002) suggests that when loss of *Nf1* predisposes Schwann cells, or their progenitors, to

upregulate EGFR, neurofibroma formation ensues. This new model will allow testing of EGFR antagonists in vivo for their ability to prevent the formation of specific phenotypes.

This study demonstrates the dramatic therapeutic effect of EGFR antagonist in mouse Schwann cells. Patients with NF1 have an increased risk of developing tumors of the central and peripheral nervous system. Among these tumors, plexiform neurofibromas are a major source of morbidity and possible mortality, with no standard treatment options other than surgery available (4, 6-8). Blockade of the EGFR receptor by its antibody has proven to be a useful strategy for the treatment of cancers including lung, breast, ovarian, head and neck cancer both *in vitro* and *in vivo*. Furthermore, some phase II and III clinical studies have also suggested that the use of mAb alone or in combination with standard anticancer therapies, are well tolerated and can induce clinical responses and tumor stabilization in a variety of carcinomas (24, 29, 36, 37) Here we described the novel targeted therapeutic effect on reversing early neurofibroma like peripheral nerve dysfunction driven by human EGFR expression in Schwann cells by using specific human mAb IMC-C225.

So what: This study further validates EGFR as a potential early target for therapeutic intervention in NF1 patients, and provides a new model in which to study early neurofibroma formation. The great potential of EGFR-targeted therapies in the treatment of many types of cancer is prompting the continued development of specific agents targeted to the extracellular ligand-binding domain, the intracellular tyrosine kinase domain, the ligand, or to synthesis of the EGFR. A SWOG trial of an EGFR tyrosine kinase inhibitor is already ongoing for MPNST (S0330 study is on OSI-774; Albritton et al., 2006). Our data suggest utility in neurofibroma as well as MPNST. Combination trials with new therapeutic drugs, such as the anti-fibrotic agent pirfenidone, and farnesyltransferase inhibitor R115777, which are now still in phase I or II clinical trial for neurofibroma might be considered. Thus our data suggest new and exciting directions in neurofibroma prevention and therapy.

References

1. Albritton, C. Rankin, C. Coffin, N. Ratner, G. T. Budd, S. Schuetze, R. L. Randall, J. DeClue, E. Borden Phase II study of Erlotinib in metastatic or unresectable malignant peripheral nerve sheath tumors (MPNST). ASCO, 2006.
2. Arteaga, C. 2003. ErbB-targeted therapeutic approaches in human cancer. *Exp Cell Res.* 284:122-130
3. Badache, A., Muja, N., and De Vries, G. (1998). Expression of Kit in neurofibromin-deficient human Schwann cells: role in Schwann cell hyperplasia associated with type 1 neurofibromatosis. Oncogene *17*, 795-800
4. Barbara, A., Burtness, Y.L., William, F., Bassam, I., and AF, A. 2002. Phase III trial comparing cisplatin(C)+placebo (P)+anti-epidermal growth factor antibody (EGFR) C225 in patient with metastatic/recurrent head & neck cancer (NHC). *Proc Am Soc Clin Oncol* 21:226a (Abstract).
5. Baselga, J., Pfister, D., Cooper, M., Cohen, R., Burtness, B., Bos, M., D'Andrea, G., Seidman, A., Norton, L., Gunnett, K., et al. 2000. Phase I studies of anti-epidermal growth factor receptor chimeric antibody C225 alone and in combination with cisplatin. *J Clin Oncol* 18:904-914
6. Blatt, J., Jaffe, R., Deutsch, M., and Adkins, J. 1986. Neurofibromatosis and childhood tumors. *Cancer* 57:1225-1229.
7. Brannan, C., Perkins, A., Vogel, K., Ratner, N., Nordlund, M., Reid, S., Buchberg, A., Jenkins, N., Parada, L., and Copeland, N. (1994). Targeted disruption of the neurofibromatosis type-1 gene leads to developmental abnormalities in heart and various neural crest-derived tissues. Genes Dev *8*, 1019-1029
8. Brown, M., and Asbury, A. (1981). Schwann cell proliferation in the postnatal mouse: timing and topography. Exp Neurol *74*, 170-186.
9. Buzard, G., Enomoto, T., Anderson, L., Perantoni, A., Devor, D., and Rice, J. (1999). Activation of neu by missense point mutation in the transmembrane domain in schwannomas induced in C3H/HeNCr mice by transplacental exposure to N-nitrosoethylurea. J Cancer Res Clin Oncol *125*, 653-659
10. Chandross, K., Cohen, R., Paras, P. J., Gravel, M., Braun , P., and Hudson, L. (1999). Identification and characterization of early glial progenitors using a transgenic selection strategy. J Neurosci *19*, 759-774
11. Chen, S., Rio, C., Ji, R., Dikkes, P., Coggeshall, R., Woolf, C., and Corfas, G. (2003). Disruption of ErbB receptor signaling in adult non-myelinating Schwann cells causes progressive sensory loss. Nat Neurosci *6*, 1186-1193
12. Ciardiello, F., and Tortora, G. 2001. A novel approach in the treatment of cancer: targeting the epidermal growth factor receptor. *Clin Cancer Res* 7:2958-2970
13. Cichowski, K., Shih, T. S., Schmitt, E., Santiago, S., Reilly, K., McLaughlin, M. E., Bronson, R. T., and Jacks, T. (1999). Mouse models of tumor development in neurofibromatosis type 1. Science *286*, 2172-2176
14. Creange, A., Zeller, J., Rostaing-Rigattieri, S., Brugieres, P., Degos, J., Revuz, J., and Wolkenstein, P. 1999. Neurological complications of neurofibromatosis type 1 in adulthood. *Brain* 122:473-481

15. Cunningham D, Humblet Y, Siena S, Khayat D, Bleiberg H, Santoro A, Bets D, Mueser M, Harstrick A, Verslype C*, et al.* (2004). Cetuximab monotherapy and cetuximab plus irinotecan in irinotecan-refractory metastatic colorectal cancer. N Engl J Med *351*, 337-345
16. DeClue, J.E., Heffelfinger, S., Benvenuto, G., Ling, B., Li, S., Rui, W., Vass, W.C., Viskochil, D., and Ratner, N. 2000. Epidermal growth factor receptor expression in neurofibromatosis type-1 related tumors and NF1 animal models. *J Clin Invest* 105:1-10.32
17. Discafani, C., Carroll, M., Floyd, M.J., Hollander, I., Husain , Z., Johnson, B., Kitchen, D., May, M., Malo, M., Minnick, A.J., et al. 1999. Irreversible inhibition of epidermal growth factor receptor tyrosine kinase with in vivo activity by N-[4-[(3-bromophenyl)amino]-6-quinazolinyl]-2-butynamide (CL-387,785). *Biochem Pharmacol.* 57:917-925
18. Evans, D., Baser, M., McGaughran, J., Sharif, S., Howard, E., and Moran, A. (2002). Malignant peripheral nerve sheath tumours in neurofibromatosis 1. J Med Genet *39*, 311-314
19. Fan, Z., Masui, H., Altas, I., and Mendelsohn, J. 1993. Blockade of epidermal growth factor receptor function by bivalent and monovalent fragments of 225 anti-epidermal growth factor receptor monoclonal antibodies. *Cancer Res.* 53:4322-4328
20. Feldkamp, M., Angelov, L., and Guha, A. (1999). Neurofibromatosis type 1 peripheral nerve tumors: aberrant activation of the Ras pathway. Surg Neurol *51*, 211-218
21. Friedman, J. 1999. Epidemiology of neurofibromatosis type 1. *Am J Med Genet* 89:1-6
22. Friedman, J., and Birch, P. (1997). Type 1 neurofibromatosis: a descriptive analysis of the disorder in 1,728 patients. Am J Med Genet *70*, 138-143
23. Garratt, A., Britsch, S., and Birchmeier, C. (2000). Neuregulin, a factor with many functions in the life of a schwann cell. Bioessays *22*, 987-996
24. Gitler, A., Zhu, Y., Ismat, F., Lu, M., Yamauchi, Y., Parada, L., and JA., E. (2003). Nf1 has an essential role in endothelial cells. Nat Genet *33*, 75-79
25. Gravel, M., Di Polo, A., Valera, P., and Braun, P. (1998). Four-kilobase sequence of the mouse CNP gene directs spatial and temporal expression of lacZ in transgenic mice. J Neurosci Res *53*, 393-404
26. Grinspan, J., Marchionni, M., Reeves, M., Coulaloglou, M., and Scherer, S. 1996. Axonal interactions regulate Schwann cell apoptosis in developing peripheral nerve: neuregulin receptors and the role of neuregulins. *J Neurosci.* 16:6107-6118.
27. Gutmann, D., Aylsworth, A., Carey, J., Korf, B., Marks, J., Pyeritz, R., Rubenstein, A., and Viskochil , D. 1997. The diagnostic evaluation and multidisciplinary management of neurofibromatosis 1 and neurofibromatosis 2. *JAMA* 278:51-57
28. Haney, C., Sahenk, Z., Li, C., Lemmon, V., Roder, J., and Trapp, B. (1999). Heterophilic binding of L1 on unmyelinated sensory axons mediates Schwann cell adhesion and is required for axonal survival. Cell Biol *146*, 1173-1184
29. Hirao, T., Sawada, H., Koyama, F., Watanabe, A., Y, Y., Sakaguchi, T., Tatsumi, M., Fujimoto, H., Emoto, K., Narikiyo, M., et al. 1999. Antisense epidermal growth factor receptor delivered by adenoviral vector blocks tumor growth in human gastric cancer. *Cancer Gene Ther* 6:423-427
30. Huang, S., Bock, J., and Harari, P. 1999. Epidermal growth factor receptor blockade with C225 modulates proliferation, apoptosis, and radiosensitivity in squamous cell carcinomas of the head and neck. *Cancer Res.* 59:1935-1940

31. Huijbregts, R., Roth, K., Schmidt, R., and Carroll, S. (2003). Hypertrophic neuropathies and malignant peripheral nerve sheath tumors in transgenic mice overexpressing glial growth factor beta3 in myelinating Schwann cells. J Neurosci *23*, 7269-728

32. Huson, S. (1998). Neurofibromatosis type 1: Historical perspective and introductory overview. in Neurofibromatosis type 1: from genotype to phenotype. In Upadhyaya M and Cooper DN (ed): pp1-13 BIOS Sci Pub Ltd, Oxfor, U K

33. Huson, S. 1994. The neurofibromatosis. Chapman ans Hall : London.

34. Jacks, T., Shih, T. S., Schmitt, E. M., Bronson, R. T., Bernards, A., and Weinberg, R. A. (1994). Tumor predisposition in mice heterozygous for a targeted mutation in NF1. Nature Genetics *7*, 353-361

35. Jessen, K., Morgan, L., Stewart, H., and Mirsky, R. (1990). Three markers of adult non-myelin-forming Schwann cells, 217c(Ran-1), A5E3 and GFAP: development and regulation by neuron-Schwann cell interactions. Development *109*, 91-103.

36. Johnson, M., Kamso-Pratt, J., Federspiel, C., and Whetsell, W. J. (1990). Mast cell and lymphoreticular infiltrates in neurofibromas. Comparison with nerve sheath tumors. Arch Pathol Lab Med *113*, 1263-1270

37. Karashima, T., Sweeney, P, Slaton, J., Kim, S., Kedar, D., Izawa, J., Fan, Z., Pettaway, C., Hicklin , D., Shuin, T., et al. 2002. Inhibition of angiogenesis by the antiepidermal growth factor receptor antibody ImClone C225 in androgen-independent prostate cancer growing orthotopically in nude mice. *Clin Cancer Res* 8:1253-1264

38. Kawamoto, T., Sato, J., Le, A., Polikoff , J., Sato, G., and Mendelsohn, J. 1983. Growth stimulation of A431 cells by epidermal growth factor: identification of high-affinity receptors for epidermal growth factor by an anti-receptor monoclonal antibody. *Proc Natl Acad Sci U S A* 80:1337-1341

39. Kim, H. A., Rosenbaum, T., Marchionni, M. A., Ratner, N., and DeClue, J. E. (1995). Schwann cells from neurofibromin deficient mice exhibit activation of $p21^{ras}$, inhibition of cell proliferation and morphological changes. Oncogene *11*, 325-335

40. Kim, H., Ratner, N., Roberts, T., and Stiles, C. 2001. Schwann cell proliferative responses to cAMP and Nf1 are mediated by cyclin D1. *J Neurosci.* 21:1110-1116

41. Krishnaswamy, G., Kelley, J., Johnson, D., Youngberg, G., Stone, W., Huang , S., Bieber , J., and Chi, D. (2001). The human mast cell: functions in physiology and disease. Front Biosci *6*, D1109-1127

42. Krof. 1999. Plexiform neurofibromas. *Am J Med Genet* 89:31-37

43. Legius, E., Marchuk, D., Collins, F., and Glover, T. (1993). Somatic deletion of the neurofibromatosis type 1 gene in a neurofibrosarcoma supports a tumor suppressor gene hypothesis. Nat Genet *3*, 122-126

44. Levi, A., Bunge, R., Lofgren, J., Meima, L., Hefti, F., Nikolics, K., and Sliwkowski, M. (1995). The influence of heregulins on human Schwann cell proliferation. J Neurosci *15*, 1329-1340

45. Li, H., Velasco-Miguel, S., Vass, W., Parada, L., and DeClue, J. 2002. Epidermal growth factor receptor signaling pathways are associated with tumorigenesis in the Nf1:p53 mouse tumor model. *Cancer Res.* 62:4507-4513

46. Ling B, Wu J, Miller S, Monk K, Shamekh R, Rizvi T, Decourten-Myers G, Vogel K, DeClue J, Ratner N: Role for the epidermal growth factor receptor in neurofibromatosis-related peripheral nerve tumorigenesis. Cancer Cell 2005, 7:65-75

47. Luetteke NC, Phillips HK, Qiu TH, Copeland NG, Earp HS, Jenkins NA, and DC, L. (1994). The mouse waved-2 phenotype results from a point mutation in the EGF receptor tyrosine kinase. Genes Dev *8*, 399-413

48. Ma, L., Gauville, C., Berthois, Y., Millot, G., Johnson, G., and Calvo, F. 1999. Antisense expression for amphiregulin suppresses tumorigenicity of a transformed human breast epithelial cell line. *Oncogene* 18:6513-6520

49. Mashour, G., Ratner, N., Khan, G., Wang, H., Martuza, R., and Kurtz, A. 2001. The angiogenic factor midkine is aberrantly expressed in NF1-deficient Schwann cells and is a mitogen for neurofibroma-derived cells. *Oncogene* 20:97-105

50. Mata, M., Alessi, D., and Fink, D. (1990). S100 is preferentially distributed in myelin-forming Schwann cells. J Neurocytol *19*, 432-442

51. Mendelsohn, J., and Baselga, J. 2000. The EGF receptor family as targets for cancer therapy. *Oncogene* 19:6550-6565

52. Michailov GV, Sereda MW, Brinkmann BG, Fischer TM, Haug B, Birchmeier C, Role L, Lai C, Schwab MH, and KA, N. (2004). Axonal neuregulin-1 regulates myelin sheath thickness. Science *304*, 700-703

53. Miller, S.J., Li, H., Rizvi, T.A., Huang, Y., Johansson, G., Bowersock, J., Sidani, A., Vitullo, J., Vogel, K., Parysek, L.M., et al. 2003. Brain lipid binding protein in axon-Schwann cell interactions and peripheral nerve tumorigenesis. *Mol Cell Biol* 23:2213-2224

54. Moasser, M., Basso, A., Averbuch, S., and Rosen, N. 2001. The tyrosine kinase inhibitor ZD1839 ("Iressa") inhibits HER2-driven signaling and suppresses the growth of HER2-overexpressing tumor cells. *Cancer Res.* 61:7184-7188

55. Morrissey, T., Levi, A., Nuijens, A., Sliwkowski, M., and Bunge, R. (1995). Axon-induced mitogenesis of human Schwann cells involves heregulin and p185erbB2. Proc Natl Acad Sci U S A *92*, 1431-1435

56. Murali, R., Brennan, P., Kieber-Emmons, T., and Greene, M. (1996). Structural analysis of p185c-neu and epidermal growth factor receptor tyrosine kinases: oligomerization of kinase domains. Proc Natl Acad Sci U S A *93*, 6252-6257

57. Needle, M., Cnaan, A., Dattilo, J., Chatten, J., Phillips, P., Shochat, S., Sutton, L., Vaughan, S., Zackai, E., Zhao, H., et al. 1997. Prognostic signs in the surgical management of plexiform neurofibroma: the Children's Hospital of Philadelphia experience, 1974-1994. *J Pediatr* 131:678-682

58. Noble ME, Endicott JA, and LN, J. (2004). Protein kinase inhibitors: insights into drug design from structure. Science *303*, 1800-1805.

59. Nutt, J., Lazarowicz, H., Mellon, J., and Lunec , J. 2004. Gefitinib ('Iressa', ZD1839) inhibits the growth response of bladder tumour cell lines to epidermal growth factor and induces TIMP2. *Br J Cancer* 90:1679-1685.

60. Packer, R., Gutmann, D., Rubenstein, A., Viskochil, D., Zimmerman, R., Vezina, G., Small, J., and Korf, B. 2002. Plexiform neurofibromas in NF1: toward biologic-based therapy. *Neurology* 58:1461-1470

61. Peng, D., Fan, Z., Lu, Y., DeBlasio, T., Scher , H., and Mendelsohn, J. 1996. Anti-epidermal growth factor receptor monoclonal antibody 225 up-regulates p27KIP1 and induces G1 arrest in prostatic cancer cell line DU145. *Cancer Res.* 56:3666-3669

62. Perry, A., Kunz, S., Fuller, C., Banerjee, R., Marley, E., Liapis, H., and Watson, M., Gutmann, DH. (2002). Differential NF1, p16, and EGFR patterns by interphase cytogenetics (FISH) in malignant peripheral nerve sheath tumor (MPNST) and morphologically similar spindle cell neoplasms. J Neuropathol Exp Neurol *61*, 702-709.

63. Plone, M., Emerich, D., and Lindner, M. 1996. Individual differences in the hotplate test and effects of habituation on sensitivity to morphine. *Pain* 66:265-270

64. Prenzel, N., Fischer, O., Streit, S., Hart, S., and Ullrich , A. (2001). The epidermal growth factor receptor family as a central element for cellular signal transduction and diversification. Endocr Relat Cancer *8*, 11-31

65. Ranson, M., Hammond, L., Ferry, D., Kris, M., Tullo, A., Murray, P., Miller, V., Averbuch, S., Ochs, J., Morris, C., *et al.* (2002). ZD1839, a selective oral epidermal growth factor receptor-tyrosine kinase inhibitor, is well tolerated and active in patients with solid, malignant tumors: results of a phase I trial. J Clin Oncol *20*, 2240-2250

66. Riccardi, V. (1992). Neurofibromatosis: phenotpye, natural history and pathogenesis, 2nd edition. p.498. John Hopkins University Press, Baltimore, MD.

67. Robert, F., Ezekiel, M., Spencer, S., Meredith, R., Bonner, J., Khazaeli, M., Saleh, M., Carey , D., LoBuglio, A., Wheeler, R., et al. 2001. Phase I study of anti--epidermal growth factor receptor antibody cetuximab in combination with radiation therapy in patients with advanced head and neck cancer. *J Clin Oncol.* 19:3234-3243

68. Salomon, D., Brandt, R., Ciardiello, F., and Normanno, N. 1995. Epidermal growth factor-related peptides and their receptors in human malignancies. *Crit Rev Oncol Hematol* 19:183-232

69. Sawada, S., Florell, S., Purandare, SM, O., M, , Stephens, K., and Viskochil, D. (1996). Identification of NF1 mutations in both alleles of a dermal neurofibroma. Nat Genet *14*, 110-112

70. Schlessinger, J. 2000. Cell signaling by receptor tyrosine kinases. *Cell* 103:211-225

71. Sclabas, G., Fujioka, S., Schmidt, C., Fan, Z., Evans, D., and Chiao, P. 2003. Restoring apoptosis in pancreatic cancer cells by targeting the nuclear factor-kappaB signaling pathway with the anti-epidermal growth factor antibody IMC-C225. *J Gastrointest Surg* 7:37-43

72. Serra, E., Puig, S., Otero, D., Gaona, A., Kruyer, H., Ars, E., Estivill , X., and Lazaro, C. (1997). Confirmation of a double-hit model for the NF1 gene in benign neurofibromas. Am J Hum Genet *61*, 512-519.

73. Shawver, L., Slamon, D., and Ullrich, A. 2002. Smart drugs: tyrosine kinase inhibitors in cancer therapy. *Cancer Cell* 1:117-123

74. Sheela, S., Riccardi, V., and Ratner, N. 1990. Angiogenic and invasive properties of neurofibroma Schwann cells. *J Cell Biol* 111:645-653

75. Sherman, L., Atit, R., Rosenbaum, T., Cox, A., and Ratner, N. (2000). Singel cell Ras-GTP analysis reveals altered Ras activity in a subpopulation of neurofibroma Schwann cells but not fibroblasts. J Biol Chem *275*, 30740-30745

76. Tsukada Y, K. T. (1992). 2', 3'-cyclic nucleotide 3'-phosphodiesterase: molecular characterization and possible functional significance. In Martenson RE(ed): Myelin: Biology and Chemistry CRC Press:Boca T|Raton, FL, 449-480.

77. Ullrich, A., and Schlessinger, J. 1990. Signal transduction by receptors with tyrosine kinase activity. *Cell* 61:203-212

78. Velu, T., Beguinot, L., Vass, W., Willingham, M., Merlino, G., Pastan, I., and Lowy, D. (1987). Epidermal-growth-factor-dependent transformation by a human EGF receptor proto-oncogene. Science *238,* 1408-1410

79. Vogel, K. S., Klesse, L. J., Velasco-Miguel, S., Meyers, K., Rushing, E. J., and Parada, L. F. (1999). Mouse tumor model for neurofibromatosis type 1. Science *286,* 2176-2179

80. Wallace, M., Andersen, L., Saulino, A., Gregory, P., Glover, T., and Collins, F. (1991). A de novo Alu insertion results in neurofibromatosis type 1. Nature *353,* 864-866

81. Wechsler, W., Rice, J., and Vesselinovitch, S. (1979). Transplacental and neonatal induction of neurogenic tumors in mice: comparison with related species and with human pediatric neoplasms. Natl Cancer Inst Monogr *51,* 219-226

82. Weissbarth, S., Maker, H., Raes, I., Brannan, T., Lapin, E., and Lehrer, G. (1981). The activity of 2',3'-cyclic nucleotide 3'-phosphodiesterase in rat tissues. J Neurochem *37,* 677-680

83. Wise, J., Patel, S., and Ahah, J. 2002. Management issues in massive pediatric facial plexiform neurofibroma with neurofibromatosis type 1. *Head Neck* 24:207-211

84. Woodruff. 1999. Pathology of tumors of the peripheral nerve sheath in type 1 neurofibromatosis. *Am J Med Genet* 89:23-30

85. Xu, G., O'Connell, P., Viskochil, D., Cawthon, R., Robertson, M., Culver, M., Dunn, D., Stevens, J., Gesteland, R., and White, R., et al. (1990). The neurofibromatosis type 1 gene encodes a protein related to GAP. Cell *62,* 599-608.

86. Yang, F., Ingram, D., Chen, S., Hingtgen, C., Ratner, N., Monk, K., Clegg, T., White, H., Mead, L., Wenning, M., et al. 2003. Neurofibromin-deficient Schwann cells secrete a potent migratory stimulus for Nf1+/- mast cells. *J Clin Invest* 112:1851-1861

87. Yang, X., Jia, X., Corvalan, J., Wang , P., Davis, C., and Jakobovits, A. 1999. Eradication of established tumors by a fully human monoclonal antibody to the epidermal growth factor receptor without concomitant chemotherapy. *Cancer Res.* 59:1236-1243.

88. Yarden, Y. (2001). The EGFR family and its ligands in human cancer. signalling mechanisms and therapeutic opportunities. Eur J Cancer *37,* S3-8.

89. Ye, D., Mendelsohn, J., and Fan, Z. 1999. Androgen and epidermal growth factor down-regulate cyclin-dependent kinase inhibitor p27Kip1 and costimulate proliferation of MDA PCa 2a and MDA PCa 2b prostate cancer cells. *Clin Cancer Res* 5:2171-2177

90. Zhu, Y., Ghosh, P., Charnay, P., Burns, D., and Parada, L. (2002). Neurofibromas in NF1: Schwann cell origin and role of tumor environment. Science *296,* 920-922.